ABSTRACT

Title of Document: FLUORESCENCE CORRELATION
                             SPECTROSCOPY STUDIES OF DNA
                             BINDING TO CATANIONIC SURFACTANT
                             VESICLES

                             Sara Bethany Lioi, Doctor of Philosophy, 2010

Directed By: Professor Douglas English, Special Member,
                             Department of Chemistry and Biochemistry
                             Professor Philip DeShong, Department of
                             Chemistry and Biochemistry

Catanionic vesicles, made from mixtures of oppositely charged surfactants, have potential in drug delivery and gene therapy applications. Fluorescence correlation spectroscopy (FCS) was utilized to study the electrostatic binding of DNA molecules to vesicles made from cetyltrimethylammonium tosylate (CTAT) and sodium dodecylbenzenesulfonate (SDBS). FCS is employed to make sensitive measurements of bilayer adsorption and compare the adsorption of two single-stranded, dye-labeled DNA molecules of different lengths. Previous experimentation had shown that small organic fluorescent dyes bind to oppositely charged vesicles, thus positively charged CTAT-rich vesicles were used in the study of DNA binding.

FCS was performed on samples with a constant DNA concentration and varying surfactant concentrations in order to construct binding isotherms for a 5mer ssDNA molecule and a 40mer ssDNA molecule. The binding constant determined

for 40mer ssDNA ($\sim 10^6$) was larger than the constant for 5mer ssDNA ($\sim 10^5$), and binding constants for both lengths of DNA were larger than those previously determined for small organic molecule fluorescent dyes, which were on the order of 10^4. Additionally, 40mer ssDNA was found to probe the critical aggregation concentration, which is the lower limit at which vesicles can form in a surfactant mixture. Ordinarily it would be expected that very few vesicles would form at this surfactant concentration, however the autocorrelation curves indicate that the 40mer is bound only to vesicles.

Salt studies were also done with the 40mer ssDNA to determine how the binding of cargo molecules to the exterior of the vesicle would be affected by physiological salt concentrations. Binding affinity of the 40mer ssDNA was reduced with increasing salt concentration; this was thought to be due to the tosylate ion, as it is hydrophobic and intercalates into the vesicle bilayer. Subsequent experiments using cetyltrimethylammonium bromide (CTAB) indicated that the counterion is not a factor in loss of binding affinity under normal saline conditions. Because these surfactant vesicles have been shown to have potential in both drug delivery and gene therapy, it is important that the binding of the cargo molecule be able to withstand normal saline conditions.

FLUORESCENCE CORRELATION SPECTROSCOPY STUDIES OF DNA
BINDING TO CATANIONIC SURFACTANT VESICLES

By

Sara Bethany Lioi

Dissertation submitted to the Faculty of the Graduate School of the
University of Maryland, College Park, in partial fulfillment
of the requirements for the degree of
Doctor of Philosophy
2010

Advisory Committee:
Professor Philip DeShong, Chair
Professor Douglas English, Co-Chair
Professor Jason Kahn
Professor Neil Blough
Professor Srinivasa Raghavan

Dedication

This work is dedicated in loving memory of my Grandmother Barbara Kay Hughes, who was always proud of me no matter what.

Acknowledgements

I would first like to thank Dr. Douglas English, my advisor, whose guidance has helped me throughout graduate school. His advice and direction has led me to become a better scientist and experimentalist. I would like to thank Dr. Philip DeShong for becoming my advisor in Dr. English's absence and adopting me into his lab. I would also like to express gratitude to my committee members Dr. Jason Kahn, Dr. Neil Blough, and Dr. Srinivasa Raghavan.

My group members Kathy Goodson, Xiang Wang, Amy Petrik, Nikolai Sinkov, Chip Luckett, and Emily Danoff were all helpful and supportive, and I would like to thank them for that. A special thank you goes to Kathy for making long hours in a pitch black room much more enjoyable and for being my friend as well as my labmate. I would also like to thank the members of the DeShong lab and the English lab in Wichita for being so kind and helpful while I was there.

I would never have made it through graduate school without the friendship and support of my fellow graduate students Melissa Resto, Kelly Daggett, Rebecca Vieira, Will Harrell, Brian Borak, Tu-Van Le Lambert, Tony Dylla, Mike Brindza, and Neil Campbell. They were always there to discuss topics scientific and otherwise, and we always managed to have a little fun even when we were stressed out.

Lastly, but certainly not least, I would like to thank my family for being so supportive and for not asking me too many times when I was going to graduate. My Mom has always been there to listen even though she thinks vesicle is a word I made up, and she has always been loving, encouraging, and supportive. My Dad instilled a

Table of Contents

List of Tables

List of Figures

List of Abbreviations

APD	avalanche photodiode
cac	critical aggregation concentration
CF	carboxyfluorescein
cmc	critical micelle concentration
CTAT	cetyltrimethylammonium tosylate
CTAB	cetyltrimethylammonium bromide
$DiIC_{18}$	1,1'-dioctadecyl-3,3,3',3'-tetramethylindocarbocyanine perchlorate
DLS	dynamic light scattering
DMEM	Dulbecco's modified eagle medium
dsDNA	double stranded deoxyribonucleic acid
FBS	fetal bovine serum
FCS	fluorescence correlation spectroscopy
mf	mole fraction
MSC	marrow stromal cell
R6G	rhodamine 6G
RAW	264.7 mouse leukemic monocyte macrophage cell line
SDBS	sodium dodecylbenzenesulfonate
ssDNA	single stranded deoxyribonucleic acid

Chapter 1: Surfactants

1.1 *Introduction*

Surfactants have many uses in detergents, paints, cosmetics, pharmaceuticals, and even in the oil industry.[1] Moreover, the aggregate structures that surfactants can form such as micelles and vesicles have many uses in the above areas and new uses continue to be proposed. For instance, surfactant vesicles have been proposed as a replacement in applications where phospholipid vesicles have traditionally been utilized; the surfactant vesicles remain stable for long periods of time of a year or more[2] in comparison to stability of a few days for phospholipid vesicles. In order to extend the usefulness of surfactant vesicle preparations, their physical properties and behavior in solutions must be considered. If surfactant vesicles are to be used in biotechnological applications, the binding or incorporation of biological molecules such as DNA will have to be studied, and some of these studies are detailed herein.

1.2 *Introduction to Physical Properties of Surfactants*

Surfactants are composed of a polar headgroup region and a nonpolar hydrophobic tail region, and can be classified into four categories: anionic, cationic, zwitterionic, and nonionic. This categorization is based on what type of headgroup the surfactant contains. The term surfactant derives from the phrase "surface active agents," which refers to one of their interesting physical properties of assembling at surfaces. Surfactants tend to assemble at surfaces or interfaces because of the nonpolar hydrophobic tail region (Fig. 1.1). They are generally soluble in water, and

assembly at surfaces, such as the air/water and solid/water interface, occurs in order to minimize contact between the hydrophobic tail region and water. This behavior results in a reduction in surface tension of solutions that contain surfactants. As the concentration of surfactant is increased in solution, there comes a point at which the surface tension no longer changes, and this point is known as the critical micelle concentration (cmc). The critical micelle concentration is the surfactant concentration at which micelles begin to form, which provides the surfactant molecules with another method of reducing contact between the hydrophobic tail region and water.[1]

Polar headgroup region   Non-polar tail region
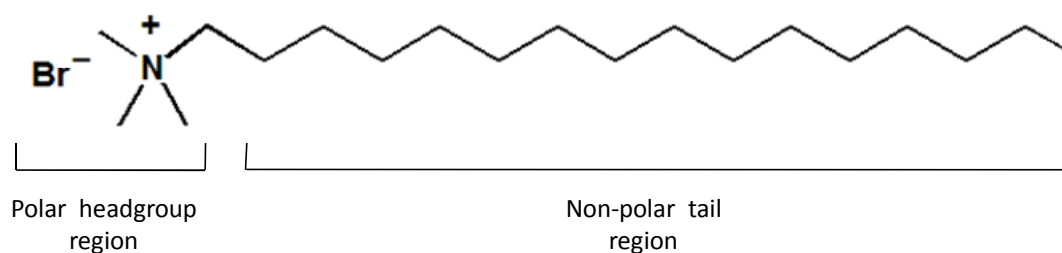
Figure 1.1 Example surfactant structure
The structure of the cationic surfactant cetyltrimethylammonium bromide as an example of a surfactant molecule showing the polar headgroup region with counterion and the hydrophobic tail region.

1.3   *Thermodynamics of Self-Assembly and CMC*

When the thermodynamics of surfactants in solution are considered, there are several opposing forces that come into play because of the amphiphilic nature of the surfactants. These forces include the hydrophobic effect, headgroup-headgroup repulsion, hydration forces, and steric effects, but the hydrophobic effect is perhaps the strongest driving force. The hydrophobic effect involves the transfer of a hydrocarbon molecule (the surfactant tail) from a polar environment to a nonpolar environment, and this process is accompanied by a reduction in free energy.[1] The

hydrophobic effect describes surfactant molecules assembling at interfaces and also assembling into larger structures such as micelles and vesicles. Below the cmc, only surfactant assembly at surfaces needs to be considered, but above the cmc, surfactants begin assembling into larger aggregates, such as micelles and vesicles, and one must consider the thermodynamics of those aggregates as well.

Surfactant micelles in solution at equilibrium can be described using the phase separation model, which treats the micelle as a separate phase wherein the chemical potential of the surfactant is assumed to be the same everywhere whether it is in solution or in a micelle.[3] An expression for the chemical potential of a surfactant molecule in water is represented as

$$\mu = \mu^\circ + RT \ln a \tag{1.1}$$

where μ° is the chemical potential in the standard state and a is the activity of the molecule in solution.[1] The activity of the surfactant a can be defined as either xf, where x is the mole fraction of the surfactant in solution and f is the activity coefficient of the surfactant, or as cf, where c is the concentration of surfactant in solution.[1] If the solution is ideal, the activity coefficient is equal to one, and the chemical potential of surfactant in solution below the cmc can be equated to

$$\mu_{monomer} = \mu^\circ_{monomer} + RT \ln C^m \tag{1.2}$$

where C^m is the concentration of the monomer in solution. In an ideal solution at or above the cmc, the chemical potential of surfactant monomer in solution can be equated to

$$\mu^*_{monomer} = \mu^\circ_{monomer} + RT \ln C^* \tag{1.3}$$

where C^* is the cmc of the surfactant. When describing a surfactant that is partitioning from the solution to a micelle, the free energy change for this process is given by

$$\Delta \bar{G} = \bar{G}_{final} - \bar{G}_{initial} = \mu_{micelle} - \mu_{monomer}.$$ (1.4)

When the system is at equilibrium, $\Delta \bar{G} = 0$, so the chemical potential of surfactant in a micelle is equal to the chemical potential of the surfactant in solution, and therefore the chemical potential of surfactant in a micelle is given by

$$\mu_{micelle} = \mu^*_{monomer} + RT \ln a.$$ (1.5)

This equation can then be combined with equation 1.3 to obtain

$$\mu_{micelle} = \mu^{\circ}_{monomer} + RT \ln C^* + RT \ln a,$$ (1.6)

and then further substituted using equation 1.2 to obtain

$$\mu_{micelle} = \mu_{monomer} - RT \ln C^m + RT \ln C^* + RT \ln a$$ (1.7)

which simplifies to give an equation relating monomer concentration to the cmc of a surfactant solution. The simplified equation is

$$C^m = C^* a$$ (1.8)

where a is the activity of the surfactant as described above. This equation is appropriate for use in surfactant solutions that have a single surfactant species and that behave ideally.[3] For non-ideal solutions, regular solution theory is applied.

1.4   *Regular Solution Theory*

Many surfactant solutions do not behave ideally because of electrostatic effects arising from charged surfactants, so regular solution theory must be used to properly model the thermodynamics of the system. Non-ideal solutions reach

equilibrium (Fig. 1.2) just as ideal solutions do, and at equilibrium the chemical potential of one surfactant species is the same whether it is in solution or in an aggregate.[3]   In an ideal solution with only one surfactant, the concentration of monomer in solution can be equated to the cmc. In non-ideal solutions containing only one surfactant, the concentration of monomer in solution is represented by equation 1.8, but in a mixed surfactant solution, the monomer concentrations must be calculated separately and the following equation is used:

$$C_i^m = x_i f_i C_i^* \tag{1.9}$$

where x_i is the mole fraction of component i in the aggregate, f_i is the activity coefficient of component i, and C_i^* is the cmc of component i.[3]
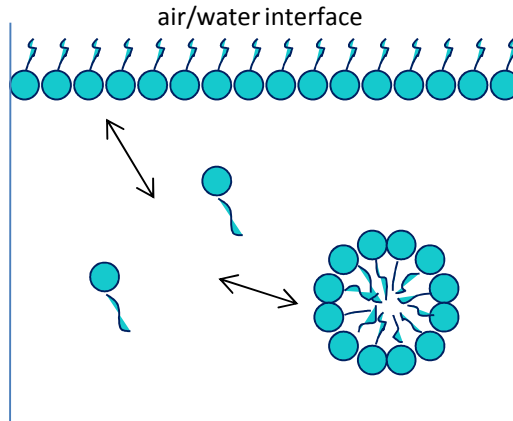
Figure 1.2 Equilibrium of surfactants in solution
Surfactants arrange at the air/water interface and into micelles and both states are at equilibrium with surfactant monomers in solution.

In mixed micellar systems, the cmc of the resulting solution is different from the cmc of either individual surfactant.   At the mixed cmc, the monomer concentration of each species in solution is given by[4]

$$C_i^m = \alpha_i C_{Mix}^* \tag{1.10}$$

5

which is derived from equation 1.9. If equations 1.9 and 1.10 are combined, the mixed cmc can be equated to the cmc's of the individual components in the aggregate:

$$\alpha_i C_{Mix}^* = x_i f_i C_i^* \tag{1.11}$$

and the mole fractions for the individual components in the aggregate can be equated to:

$$x_i = \frac{\alpha_i C_{Mix}^*}{f_i C_i^*} \tag{1.12}$$

For a binary surfactant mixture, the sum of the individual mole fractions of the surfactants is equal to one, and can also be equated to:

$$x_1 + x_2 = \frac{\alpha_1 C_{Mix}^*}{f_1 C_1^*} + \frac{\alpha_2 C_{Mix}^*}{f_2 C_2^*} = 1 \tag{1.13}$$

and from there, the mixed cmc can be calculated using the following equation:[3]

$$\frac{1}{C_{Mix}^*} = \frac{\alpha_1}{f_1 C_1^*} + \frac{\alpha_2}{f_2 C_2^*} \tag{1.14}$$

where C_{Mix}^* is the mixed cmc, α_1 and α_2 are the total mole fractions of the two components in solution, C_1^* and C_2^* are the cmc's of each surfactant in solution, and f_1 and f_2 are the activity coefficients of each surfactant. For an ideal solution, the activity coefficients are one, and the mixed cmc can easily be calculated; however, for a non-ideal solution, the activity coefficients must be calculated to determine the mixed cmc.[3]

The activity coefficients for non-ideal solutions are generally less than one, and the farther the solution deviates from ideality, the smaller the activity coefficient becomes. The activity coefficient is related to the type of surfactants used in the mixture; the smaller the ionic character of the surfactant is, the closer the value of the

activity coefficient for that surfactant is to one. To calculate the activity coefficient, a dimensionless interaction parameter is needed, and for a system with only two components, the activity coefficient can be determined as follows:

$$f_1 = \exp \beta \ (1 - x_1)^2 \tag{1.15}$$

$$f_2 = \exp \beta \ x_1{}^2 \tag{1.16}$$

where x_1 is the mole fraction of component 1 in the aggregate and β is the interaction parameter between the two surfactants. In binary mixtures with a strong attraction between the two surfactant species, the surfactant solution deviates farther from ideality, and the value of β becomes more negative. When β is negative, the values of the activity coefficients are lower, and the mixed cmc becomes lower in comparison to the individual cmc's of the individual surfactants in solution.[3]

1.5   *Critical Packing Parameter*
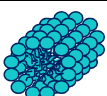
In addition to using thermodynamics to describe surfactant solutions, geometric constraints can be used to better predict what type of aggregate structure will form in a particular surfactant solution. The geometric constraints take into account the basic geometry of the surfactants themselves. The surfactants can be assigned a critical packing parameter, P, which is related to the shape of the surfactant molecule as follows:

$$P = \frac{v}{a_0 l_c} \tag{1.17}$$

where v is the volume of the hydrocarbon chain, a_0 is the area of the headgroup, and l_c is the critical hydrocarbon tail length. The tail volume can be approximated in units of Å^3 by using $(27.4 + 26.9n)$, where n is the number of carbon atoms in the

hydrophobic tail, and the tail length can be approximated in units of Å by using $(1.5 + 1.265n)$.[5] The headgroup area can be calculated using $a_0 = \sqrt{C/\gamma}$ where C is a constant in which repulsive interactions are taken into account and γ is the surface tension.[6] The headgroup area can also be determined experimentally using the Langmuir trough method.[7]

The packing parameter ranges from values of 1/3 to greater than 1, and different values for the packing parameter predict different types of aggregate structures. Values of packing parameters and the aggregate that will most likely form are shown in Table 1.1. Surfactants with a single tail tend to form spherical micelles or rod-like micelles, and surfactants with two hydrocarbon tails form bilayers.[5] One example of a single tailed surfactant that forms spherical micelles in solution is cetyltrimethylammonium bromide (CTAB),[8] and one example of a single tailed surfactant that forms rod-like or wormlike micelles in solution is cetyltrimethylammonium tosylate (CTAT).[9] The only difference between these two surfactants is the counterion, and that accounts for the difference in aggregate structure formed. In CTAT solutions, the tosylate counterion intercalates in between the CTA^+ ions so that charge screening occurs and the CTA^+ headgroups are brought closer together, reducing the average headgroup area and increasing the packing parameter.[9] For CTAB solutions, the bromide counterion does not intercalate and the headgroups repel each other, giving rise to a larger headgroup area and smaller packing parameter.[8]

Packing Parameter	Surfactant Shape		Aggregate Structure Predicted	
>1	inverted truncated cone		reverse micelle	
1/2 -1	cylinder		vesicle/ bilayer	
1/3 -1/2	truncated cone		rod-like micelle	
<1/3	cone		spherical micelle	

Table 1.1 Packing parameter values and aggregates formed
Possible packing parameter values, the shape of the surfactant associated with that packing parameter, and the structure most likely to form are shown for each value. Adapted from reference 5.

1.6   *CMC and Critical Packing Parameter in Formation of Catanionic Vesicles*

In this work, the surfactant solution of interest is one in which catanionic vesicles form; catanionic vesicles are composed of a mixture of a cationic surfactant and an anionic surfactant.   These studies focus on one particular vesicle forming system, the cetyltrimethylammonium tosylate (CTAT) and sodium dodecylbenzenesulfonate (SDBS) system.   In certain mass ratios where one of the surfactants is in excess, vesicles can form spontaneously when the two surfactants are mixed together in solution.[2] Vesicles in this system form above the mixed cmc, also referred to as the critical aggregation concentration (cac), which can be calculated using regular solution theory or determined experimentally.   The cac is much lower for a mixture of CTAT and SDBS than the pure cmc's of each component because the interaction parameter β has a very negative value of -24 for CTAT and SDBS.[10] Values for β in other catanionic systems are similar; these systems have the largest,

9

most negative values compared to other types of mixed surfactant systems. For example, anionic/nonionic systems have small negative values of β that range from -1 to -5.[3]

The anionic and cationic surfactants form an ion pair that is similar to a phospholipid because the ion pair has a single headgroup with two hydrocarbon chains (Fig. 1.3). The opposing charges of the cationic and anionic surfactant are essentially neutralized when they are paired, and it has a packing parameter of ≈1 which corresponds to a planar bilayer. For catanionic surfactant vesicles to form, one of the surfactants has to be in excess, so the excess surfactant molecules have a packing parameter of ≈1/3 in solution, which generally indicates micelle formation. Combining these two packing parameters points to a lamellar structure with the curvature of a micelle; the result is vesicle formation. The outer leaflet of the bilayer contains more of the excess surfactant, so there is non-ideal mixing between the two bilayers in order for vesicles to form. With non-ideal mixing between the bilayers, more CTA^+ is in the outer leaflet, and these CTA^+ ions repel each other, giving rise to a larger distance between headgroups and a larger curvature.[11]
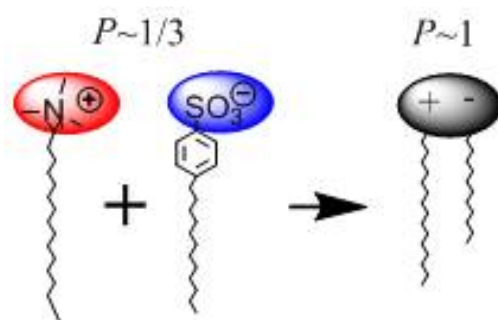
Figure 1.3 Ion pair formation
The surfactants cetyltrimethylammonium and dodecylbenzenesulfonate combine to form an ion pair similar to the structure of a phospholipid.

References

1. Tadros, T. F., *Surfactants*. Academic Press, Inc.: New York, 1984.

2. Kaler, E. W.; Murthy, A. K.; Rodriguez, B. E.; Zasadzinski, J. A. N., Spontaneous vesicle formation in aqueous mixtures of single-tailed surfactants. *Science* **1989,** 245, (4924), 1371-1374.

3. Holland, P. M., Modeling mixed surfactant systems: Basic introduction. In *Mixed surfactant systems*, Holland, P. M.; Rubingh, D. N., Eds. American Chemical Society: Washington, D.C., 1992; pp 31-44.

4. Holland, P. M.; Rubingh, D. N., Nonideal multicomponent mixed micelle model. *J. Phys. Chem.* **1983,** 87, (11), 1984-1990.

5. Israelachvilli, J. N.; Mitchell, D. J.; Ninham, B. W., Theory of self-assembly of hydrocarbon amphiphiles into micelles and bilayers. *J. Chem. Soc., Faraday Trans. 2* **1976,** 72, (9), 1525-1568.

6. Israelachvili, J. N.; Mitchell, D. J.; Ninham, B. W., Theory of self-assembly of lipid bilayers and vesicles. *Biochim. Biophys. Acta* **1977,** 470, (2), 185-201.

7. Pashley, R. M.; Karaman, M. E., *Applied colloid and surface chemistry*. John Wiley and Sons, Ltd.: New York, 2004.

8. Shikata, T.; Hirata, H.; Kotaka, T., Micelle formation of detergent molecules in aqueous-media - Viscoelastic properties of aqueous cetyltrimethylammonium bromide solutions. *Langmuir* **1987,** 3, (6), 1081-1086.

9.   Soltero, J. F. A.; Puig, J. E.; Manero, O., Rheology of the
       cetyltrimethylammonium tosilate-water system 2. Linear viscoelastic regime.
       Langmuir **1996,** 12, (11), 2654-2662.

10.   Chiruvolu, S.; Israelachvili, J. N.; Naranjo, E.; Xu, Z.; Zasadzinski, J. A.;
       Kaler, E. W.; Herrington, K. L., Measurement of forces between spontaneous
       vesicle-forming bilayers. *Langmuir* **1995,** 11, (11), 4256-4266.

11.   Safran, S. A.; Pincus, P.; Andelman, D., Theory of spontaneous vesicle
       formation in surfactant mixtures. *Science* **1990,** 248, (4953), 354-356.

Chapter 2:   Catanionic Surfactant Vesicles

2.1   *Comparison with Conventional Vesicles*

Phospholipid vesicles were first reported in the 1960's[1,2] based on visual evidence from electron microscopy studies.[1] Initial phospholipid vesicles consisted of concentric bilayers, also known as multilamellar vesicles.[1] Later studies utilized unilamellar vesicles which were formed using techniques such as sonication[3] and extrusion.[4,5] Because synthetic phospholipid vesicles are analogous to vesicles used for transport in living cells, they have been used as cell membrane models[2] and for drug delivery purposes.[6] Vesicles formed from phospholipids are very useful, however there are drawbacks to their use. Because unilamellar vesicles are formed using some sort of external energy or force, these vesicles are kinetically trapped structures and are not very stable. The vesicles tend to rupture or fuse with other vesicles in solution, which causes them to release their cargo molecules. In addition to losing their cargo molecules because of instability, the initial efficiency of encapsulating cargo molecules is low. Finally, the phospholipids used to form the vesicles are expensive. For these reasons, surfactant vesicles have been proposed as a replacement for phospholipid vesicles. Surfactant vesicles have been shown to remain stable for long periods of time[7], have recently been shown to have high encapsulation efficiencies with charged molecules,[8,9] and are relatively inexpensive compared to phospholipids.

2.2 *Background on Surfactant Vesicles*

Surfactant preparations have recently been shown to have potential in drug delivery and DNA delivery to cells,[10] but initial research into the field of catanionic surfactant vesicles focused more on their phase behavior and physical properties. Catanionic vesicles, formed from mixtures of cationic and anionic surfactants, were first reported by Kaler et al. in 1989.[7] These vesicles formed spontaneously and were reported to remain stable for at least a year.[7] Following this discovery, many more vesicle forming catanionic systems were reported, and more continue to be discovered.[11-13] The focus of this thesis is on the first system reported by Kaler et al., that of the cetyltrimethylammonium tosylate (CTAT) and sodium dodecylbenzenesulfonate (SDBS) vesicle-forming system (Figure 2.1).[7]
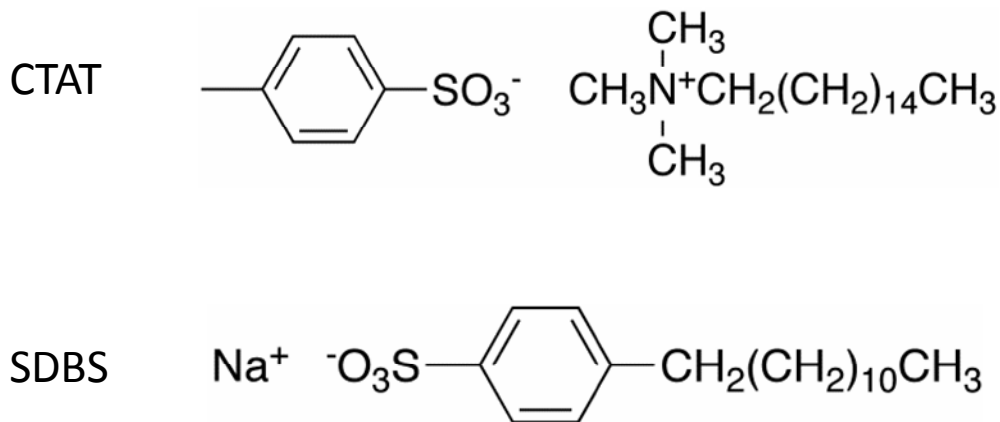
Figure 2.1 Structures of CTAT and SDBS

This first study and subsequent studies focused on the phase behavior of different mixtures of CTAT and SDBS. The phase diagram, represented in Figure 2.2, illustrates the important features of vesicle-forming catanionic mixtures. There is a precipitation zone near equimolarity, which is a result of CTA^+ and DBS^- forming ion pairs; these ion pairs have a packing parameter of ~1, so planar bilayers form

which precipitate out of solution. The two lobe-shaped regions denoted V^+ and V^- are the regions in which spontaneous vesicle formation occurs, and it indicates that stable catanionic vesicles always require one of the surfactants to be present in excess. In the case of CTAT and SDBS, the lobes extend maximally at CTAT/SDBS weight ratios of 70/30 (V^+) and 30/70 (V^-),[7, 14-16] and because of this, CTAT/SDBS vesicles are most often prepared at these surfactant ratios. In addition to phase studies, these vesicles have been analyzed using DLS,[7,16] freeze fracture TEM,[7,15,16] and cryo-TEM[15,17] to determine the radius and distribution of aggregates formed. The average radius of the vesicles ranged from 30 to 80 nm, depending on the ratio of the two surfactants, and the vesicles have either an overall positive (CTAT-rich) or negative charge (SDBS-rich).[7] This gives the bilayer a net charge that is responsible for the remarkable colloidal stability of these systems; these vesicles do not fuse together like phospholipid vesicles do over time.[15] Because of the remarkable long-term stability of these catanionic surfactant vesicles, they have been proposed for use in many biotechnological applications.
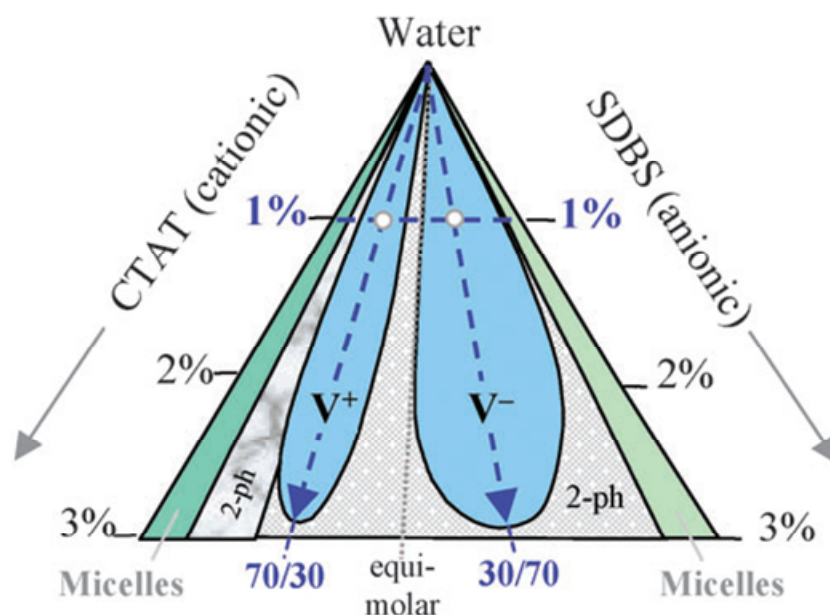
Figure 2.2 Ternary phase diagram for CTAT/SDBS solutions
The water rich corner of the phase diagram is represented where the lobes labeled V^+ and V^- indicate mixtures where vesicles form. The 2-phase region on the left consists of micelles and vesicles in coexistence, and the 2-phase region on the right consists of a lamellar phase in coexistence with vesicles. The micelle region on the left consists of worm-like micelles and the micelle region on the right consists of spherical micelles. Adapted from reference 14.

2.3 *Encapsulation with Catanionic Surfactant Vesicles*

If catanionic surfactant vesicles are to be used in applications where encapsulation of solutes is needed, the encapsulation efficiency must be studied. Since the first report of formation of catanionic vesicles in 1989, surprisingly little work has been done to study the ability of these vesicles to entrap solutes. In the initial work by Kaler et al. with catanionic vesicles formed from CTAT and SDBS, it was reported that the vesicles were able to encapsulate glucose, but no quantitative data was reported.[7] Later, Kondo et al. studied glucose entrapment in a different catanionic vesicle system, with vesicles formed from the surfactants didodecyldimethylammonium bromide (DDAB) and sodium dodecyl sulfate (SDS).

16

They reported a maximum encapsulation of ~ 7.9% of the initial glucose solution.[12] Bhattacharya studied vesicles formed from hybrid (bolaphile/amphiphile) ion-pairs and found that they were able to entrap riboflavin, but only with 1-2% encapsulation values.[18]

In recent years, Tondre et al. have worked extensively with catanionic vesicle systems and have tried to quantify the encapsulation of various probe molecules. In 2000, they reported that vesicles formed from the surfactants cetyltrimethylammonium bromide (CTAB) and sodium octylsulfate (SOS) were able to entrap glucose (~1%) and riboflavin (0.4%) but failed at their attempt to show entrapment of the ionic dye, carboxyfluorescein.[11] Subsequently, they reported that vesicles formed in Kaler's CTAT/SDBS system were able to entrap glucose, with encapsulation values of 1-2%. Interestingly, SDBS- rich (V^-) vesicles were able to entrap more glucose than CTAT-rich (V^+) vesicles. It was also reported that the vesicles were highly permeable and had very low long-term encapsulation, with the V^+ vesicles being substantially more leaky than the V^- vesicles.[19] Overall, the results up to this point concerning catanionic vesicles showed low, unremarkable levels of initial and long-term encapsulation, and this type of vesicle did not appear to be more efficient encapsulating solutes than conventional liposomes.

In contrast to the previous studies discussed above, recent work done in our lab explored the ability of catanionic surfactant vesicles to capture and retain small, charged solutes and found remarkably high encapsulation efficiencies for these molecules.[8,9] This work commenced with the discovery by Wang et al. that CTAT-rich vesicles (V^+), from the CTAT/SDBS system were able to sequester the dye 5(6)-

carboxyfluorescein (CF) to a much higher degree than uncharged phospholipid vesicles.[9] The apparent encapsulation efficiency ε measured by size exclusion chromatography (SEC) was 22% for V^+ and only 1.6% for EYPC vesicles. The quantity ε is referred to as the "apparent" encapsulation efficiency because it has been shown that its measured value is nearly identical regardless of whether dye addition occurs during or after vesicle formation. Adding the solute to pre-formed vesicles decreases the value of ε by only about 30%. The results indicate that molecular "encapsulation" by catanionic vesicles of oppositely charged solutes is due largely to adsorption of molecules to the vesicle exterior through electrostatic interactions with the excess surfactant present in the bilayer.[9] Additional studies with several different fluorescent dye molecules had apparent encapsulation efficiencies ranging from 20-75% and are shown in Table 2.1.[8]

	Dye Sequestration	
Probe Molecule	CTAT-rich V^+	SDBS-rich V^-
Carboxyfluorescein (CF)	24 ± 4%	1.0 ± 0.4%
Lucifer Yellow (LY)	40 ± 20%	4%
Sulforhodamine 101 (SR101)	32.8%	8.2%
Rhodamine 6G (R6G)	0.07 ± 0.1%	72 ± 3%
Doxorubicin	0%	55%

Table 2.1 Dye sequestration with CTAT-rich and SDBS-rich vesicles
Dye sequestration was measured by analyzing the amount of dye that elutes with vesicles during size exclusion chromatography. The initial dye concentration is 1.0 mM. The dyes CF, LY, and SR101 have a negative charge, and the dyes R6G and Doxorubicin have a positive charge. From reference 8.

2.4   *Surfactant Vesicles and DNA*

For surfactant vesicles to be useful in gene therapy and other DNA-related biotechnological applications, the binding of DNA to surfactant vesicles must be understood. Early experiments of DNA binding to bilayers was studied using synthetic cationic lipids, and it was found that more rigid membranes induced a larger change in the DNA conformation[20] and possibly induced strand separation.[21] Surfactant vesicles have also been used to induce a conformational change to DNA; for very long double stranded DNA, catanionic surfactant vesicles compacted the DNA from a long coil to a small globule formation.[22-24] The compaction of DNA is thought to be important in the uptake of DNA through cell membranes,[10,23] and because high concentrations of surfactants are known to be toxic to cells, amino acid based surfactants have been utilized as well.[25,26] Until now, no quantitative measure of DNA binding to catanionic surfactant vesicles has been made, and only very long double stranded DNA greater than 500 base pairs has been studied. The studies presented in this thesis include quantitative measurements of shorter double and single stranded DNA binding to CTAT/SDBS vesicles using a very sensitive technique known as fluorescence correlation spectroscopy.

References

1. Bangham, A. D.; Horne, R. W., Negative staining of phospholipids and their structural modification by-surface active agents as observed in electron microscope. *J. Mol. Biol.* **1964,** 8, (5), 660-668.

2. Bangham, A. D.; Standish, M. M.; Watkins, J. C., Diffusion of univalent ions across lamellae of swollen phospholipids. *J. Mol. Biol.* **1965,** 13, (1), 238-252.

3. Papahadjopoulos, D., Phospholipid model membranes 3. Antagonistic effects of Ca^{2+} and local anesthetics on permeability of phosphatidylserine vesicles. *Biochim. Biophys. Acta* **1970,** 211, (3), 467-477.

4. Hope, M. J.; Bally, M. B.; Webb, G.; Cullis, P. R., Production of large unilamellar vesicles by a rapid extrusion procedure - characterization of size distribution, trapped volume and ability to maintain a membrane-potential. *Biochim. Biophys. Acta* **1985,** 812, (1), 55-65.

5. Macdonald, R. C.; Macdonald, R. I.; Menco, B. P. M.; Takeshita, K.; Subbarao, N. K.; Hu, L. R., Small-volume extrusion apparatus for preparation of large, unilamellar vesicles. *Biochim. Biophys. Acta* **1991,** 1061, (2), 297-303.

6. Poznansky, M. J.; Juliano, R. L., Biological approaches to the controlled delivery of drugs - A critical review. *Pharmacol. Rev.* **1984,** 36, (4), 277-336.

7. Kaler, E. W.; Murthy, A. K.; Rodriguez, B. E.; Zasadzinski, J. A. N., Spontaneous vesicle formation in aqueous mixtures of single-tailed surfactants. *Science* **1989,** 245, (4924), 1371-1374.

8.   Danoff, E. J.; Wang, X.; Tung, S. H.; Sinkov, N. A.; Kemme, A. M.; Raghavan, S. R.; English, D. S., Surfactant vesicles for high-efficiency capture and separation of charged organic solutes. *Langmuir* **2007,** 23, (17), 8965-8971.

9.   Wang, X.; Danoff, E. J.; Sinkov, N. A.; Lee, J.-H.; Raghavan, S. R.; English, D. S., Highly efficient capture and long-term encapsulation of dye by catanionic surfactant vesicles. *Langmuir* **2006,** 22, (15), 6461-6464.

10.   Bramer, T.; Dew, N.; Edsman, K., Pharmaceutical applications for catanionic mixtures. *J. Pharm. Pharmacol.* **2007,** 59, (10), 1319-1334.

11.   Caillet, C.; Hebrant, M.; Tondre, C., Sodium octyl sulfate/cetyltrimethylammonium bromide catanionic vesicles: Aggregate composition and probe encapsulation. *Langmuir* **2000,** 16, 9099-9102.

12.   Kondo, Y.; Uchiyama, H.; Yoshino, N.; Nishiyama, K.; Abe, M., Spontaneous vesicle formation from aqueous-solutions of didodecyldimethylammonium bromide and sodium dodecyl-sulfate mixtures. *Langmuir* **1995,** 11, (7), 2380-2384.

13.   Tondre, C.; Caillet, C., Properties of the amphiphilic films in mixed cationic/anionic vesicles: A comprehensive view from a literature analysis. *Adv. Colloid Interf. Sci* **2001,** 93, 115-134.

14.   Koehler, R. D.; Raghavan, S. R.; Kaler, E. W., Microstructure and dynamics of wormlike micellar solutions formed by mixing cationic and anionic surfactants. *J. Phys. Chem. B* **2000,** 104, (47), 11035-11044.

15. Chiruvolu, S.; Israelachvili, J. N.; Naranjo, E.; Xu, Z.; Zasadzinski, J. A.; Kaler, E. W.; Herrington, K. L., Measurement of forces between spontaneous vesicle-forming bilayers. *Langmuir* **1995,** 11, (11), 4256-4266.

16. Kaler, E. W.; Herrington, K. L.; Murthy, A. K.; Zasadzinski, J. A. N., Phase-behavior and structures of mixtures of anionic and cationic surfactants. *J. Phys. Chem.* **1992,** 96, (16), 6698-6707.

17. Yaacob, II; Bose, A., An investigation of microstructures in cationic/anionic surfactant suspensions by cryogenic transmission electron microscopy. *J. Colloid Interf. Sci.* **1996,** 178, (2), 638-647.

18. Bhattacharya, S.; De, S. M.; Subramanian, M., Synthesis and vesicle formation from hybrid bolaphile/amphiphile ion-pairs. Evidence of membrane property modulation by molecular design. *J. Org. Chem.* **1998,** 63, (22), 7640-7651.

19. Fischer, A.; Hebrant, M.; Tondre, C., Glucose encapsulation in catanionic vesicles and kinetic study of the entrapment/release processes in the sodium dodecyl benzene sulfonate/cetyltrimethylammonium tosylate/water system. *J. Colloid Interf. Sci.* **2002,** 248, (1), 163-168.

20. Akao, T.; Fukumoto, A.; Ihara, H.; Ito, A., Conformational change in DNA induced by cationic bilayer membranes. *FEBS Lett.* **1996,** 391, (1-2), 215-218.

21. Kikuchi, I. S.; Carmona-Ribeiro, A. M., Interactions between DNA and synthetic cationic liposomes. *J. Phys. Chem. B* **2000,** 104, (13), 2829-2835.

22. Dias, R. S.; Lindman, B.; Miguel, M. G., Compaction and decompaction of DNA in the presence of catanionic amphiphile mixtures. *J. Phys. Chem. B* **2002,** 106, (48), 12608-12612.

23. Dias, R. S.; Pais, A.; Miguel, M. G.; Lindman, B., DNA and surfactants in bulk and at interfaces. *Colloids Surf., A* **2004,** 250, (1-3), 115-131.

24. Mel'nikov, S. M.; Dias, R.; Mel'nikova, Y. S.; Marques, E. F.; Miguel, M. G.; Lindman, B., DNA conformational dynamics in the presence of catanionic mixtures. *FEBS Lett.* **1999,** 453, (1,2), 113-118.

25. Rosa, M.; Miguel, M. D.; Lindman, B., DNA encapsulation by biocompatible catanionic vesicles. *J. Colloid Interf. Sci.* **2007,** 312, (1), 87-97.

26. Rosa, M.; Moran, M. D.; Miguel, M. D.; Lindman, B., The association of DNA and stable catanionic amino acid-based vesicles. *Colloids Surf., A* **2007,** 301, (1-3), 361-375.

Chapter 3: Fluorescence Correlation Spectroscopy

3.1   *Origin and Theory of Fluorescence Correlation Spectroscopy*

Fluorescence correlation spectroscopy (FCS) is a technique that evolved from dynamic light scattering (DLS).[1] DLS measures the intensity of light scattered by a sample at a fixed angle from the incident light (Figure 3.1) and the general autocorrelation function for DLS is[2]

$$G(\tau) = \langle I(t) \cdot I(t + \tau) \rangle. \tag{3.1}$$

DLS can be used to determine the diffusion coefficient of a chemical species in solution if the species is smaller than the wavelength of the incident light. DLS has limitations, however, when applied to measuring the kinetics of a chemical reaction if the chemicals involved in the reaction are all of a similar size. If they are all similar in size, the difference in light scattering is very small, and reaction kinetics cannot be measured.[3]
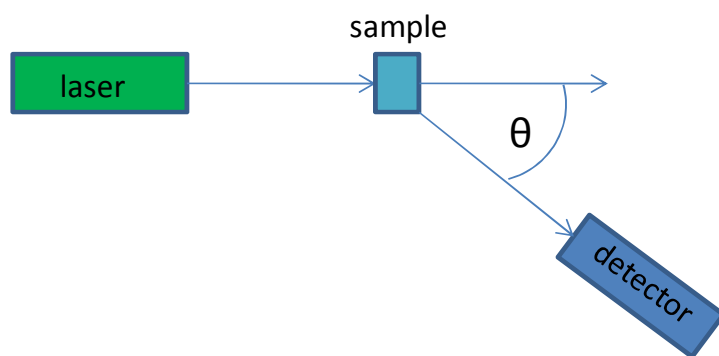
Figure 3.1 Basic schematic of DLS experimental setup
The laser hits the sample and the intensity of scattered light is measured at an angle θ from the incident light.

Fluorescence intensities are much larger than the scattering intensities measured using DLS, so if a fluorescent species is used to monitor a reaction with similarly sized molecules, reaction kinetics can be determined. The technique of FCS uses this idea of measuring fluorescence intensities combined with the general theory behind DLS. FCS is done at low concentrations so that deviations from ideality will be small and that fluctuations in fluorescence intensities will be significant, and this illustrates one of the advantages of FCS over DLS because much smaller concentrations can be used as well as smaller sample volumes. FCS can monitor reactions at equilibrium by measuring fluorescence intensity fluctuations of molecules diffusing in and out of a laser focal volume in solution, and can also measure diffusion coefficients of chemical species in solution.[2] The first FCS experiment performed measured the kinetics of the binding of ethidium bromide, a fluorescent molecule, to DNA.[1]
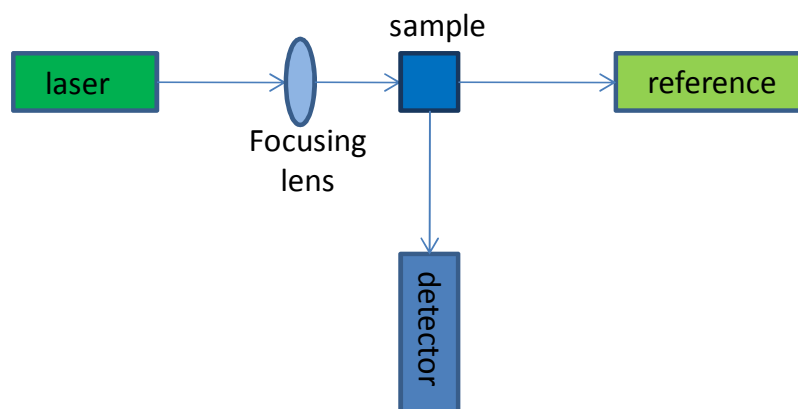
Figure 3.2 Initial setup of FCS experiments
The laser is focused into the sample and the fluorescence is detected at a 90° angle.

For this first FCS experiment, the laser was focused into solution using a lens, and a focal spot with a width on the order of micrometers was produced (Figure 3.2).[1,2] The fluorescence intensity of molecules diffusing in and out of the focal

volume was measured, and the correlation of the laser intensity fluctuation was used to determine diffusion coefficients and kinetics.[1] The fluctuation in fluorescence intensity is $\delta F(t)$, and can be represented as the fluctuations of the fluorescence intensity $F(t)$ around the average fluorescent intensity $\langle F(t) \rangle$. The fluorescence intensity fluctuations are autocorrelated and normalized according to the following generalized equation:

$$G(\tau) = \langle \delta F(t)\delta F(t+\tau)\rangle / \langle F(t)\rangle^2 \qquad (3.2)$$

and the resulting autocorrelation can be analyzed to determine diffusion coefficients and kinetic information.[4] As shown in Figure 3.3, smaller fluorescent molecules diffusing through a laser beam will have a faster autocorrelation decay, and larger fluorescent molecules diffusing through a laser beam will have a slower autocorrelation decay.
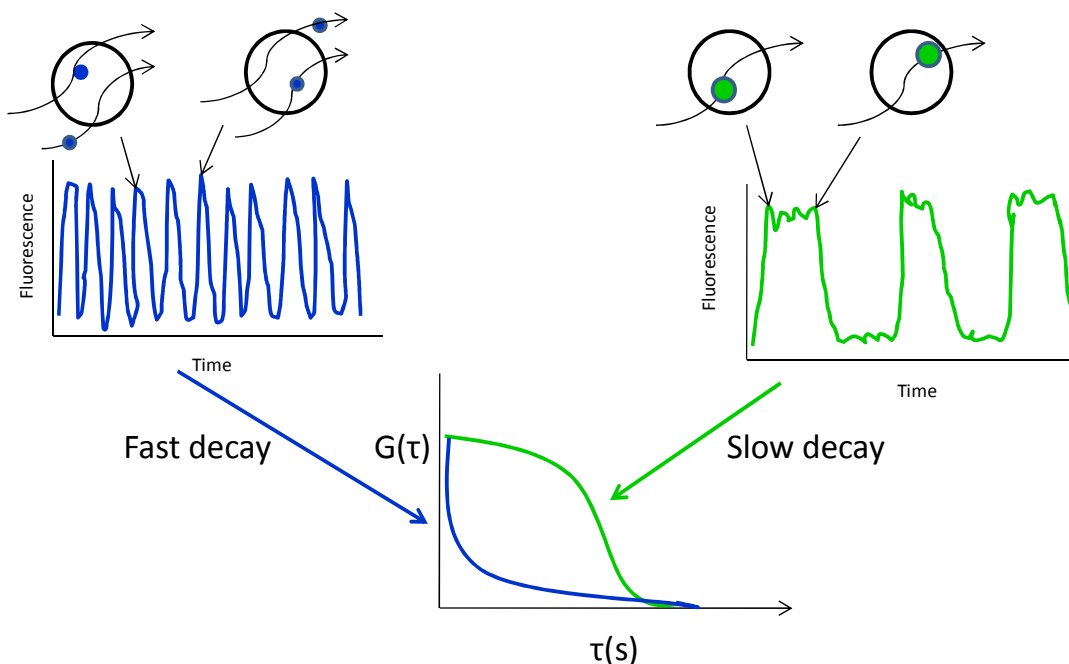
Figure 3.3 Example autocorrelation decays for a small molecule and a large molecule
A small molecule will have a faster autocorrelation decay because it diffuses more quickly through the laser beam. A large molecule will have a slower autocorrelation decay because it diffuses more slowly through the laser beam.

26

When the laser beam is focused in solution, it has a Gaussian beam profile (Figure 3.4), so the analytical treatment for FCS autocorrelation is different than that used for DLS autocorrelation.[5] Because the laser beam is focused into a small volume in the sample, this must be taken into account for the autocorrelation function, which can be approximated for one species in solution as

$$G(\tau) = (1 + \tau/\tau_D)^{-1}. \tag{3.3}$$

In this equation τ_D, the diffusion time for the molecule, is equal to $\omega^2/4D$, where ω^2 is proportional to the ratio of the radial axis to the axial axis of the focal volume and D is the diffusion coefficient of the chemical species being detected.[1] This equation, however, does not account for all processes occurring in solution that affect the detection of fluorescence such as chemical reactions, rotational diffusion, and translational diffusion.[6] A more specific equation for the autocorrelation of a single species diffusing through the focal volume is

$$G(\tau) = \frac{1}{N} * \left(\frac{1}{1+\frac{\tau}{\tau_D}}\right) * \left(\frac{1}{1+\omega^2 \frac{\tau}{\tau_D}}\right)^{\frac{1}{2}} \tag{3.4}$$

where N is the average number of molecules in the observation volume, and ω^2 and τ_D are described above.[6,7]
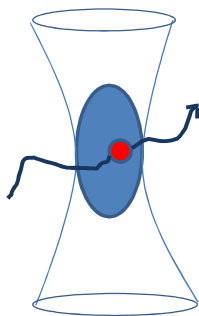
Figure 3.4 Gaussian beam profile
When the laser beam is focused into the sample solution using a microscope objective, the resulting focal volume is approximately 1 femtoliter.

3.2 Advances and Uses of FCS

Shortly after FCS was first described in the 1970's,[1] an advancement was made in the experimental set-up. A microscope was employed to focus laser light into the sample volume,[8] rather than the simple lens used in the first experiments.[1,2] The introduction of the microscope to FCS allowed for a very small focal volume of about one femtoliter, and it led to the typical experimental set-up using a confocal microscope which is used today.[7,9,10] Using a very small concentration of molecules combined with the very small focal volume, one can achieve single molecule sensitivity.[7] Other advancements such as autocorrelator electronics, increased laser stability, and avalanche photodiodes have helped make FCS an even more sensitive technique.[10]

FCS has been used for many different purposes such as measuring kinetics,[11,12] photophysical properties,[13-16] and pH sensitivity.[11,16,17] Significant focus has been placed on biological systems as well,[4] and FCS has been performed at or near bilayers and cell surfaces.[18-21] The binding of proteins to larger structures such as vesicles,[22] model bilayers,[23] and nanospheres[19] has also been investigated using FCS. Biological molecules such as proteins and DNA can be difficult to obtain and purify, so large quantities may not be available for experimentation. Utilizing FCS in studies of biological molecules has an advantage because high concentrations are not needed for this technique. In this dissertation, the binding of DNA molecules to catanionic surfactant vesicles is examined using the time tagged method of data collection.

3.3   Time-Tagged Method

In traditional FCS, the fluorescence intensity is recorded as a function of time, and this data is autocorrelated and analyzed. An acquisition time is set for data collection, and in each time period, the number of photons that reach the detector is recorded. Because very low concentrations are used in FCS experiments, the resulting data contains many data points with a value of zero. This increases the size of the data file that then has to be autocorrelated. With the time tagged method, the amount of time between photons reaching the detector is recorded, and this reduces the file size because every data point has a non-zero value. With the time-tagged method, each photon that reaches the detector is assigned an arrival time, and a trajectory of delay times is constructed (Figure 3.5). In addition to having the advantage of reduced file size, utilizing the time-tagged method of data acquisition can also provide smaller time scales for experimentation. As seen in Figure 3.5, the traditional FCS data autocorrelation has a time resolution of milliseconds, but the time-tagged data autocorrelation has microsecond time resolution. The time-tagged method can also increase the signal-to-noise ratio, reducing the amount of background fluorescence that arises from light scattering in the solvent.[24]
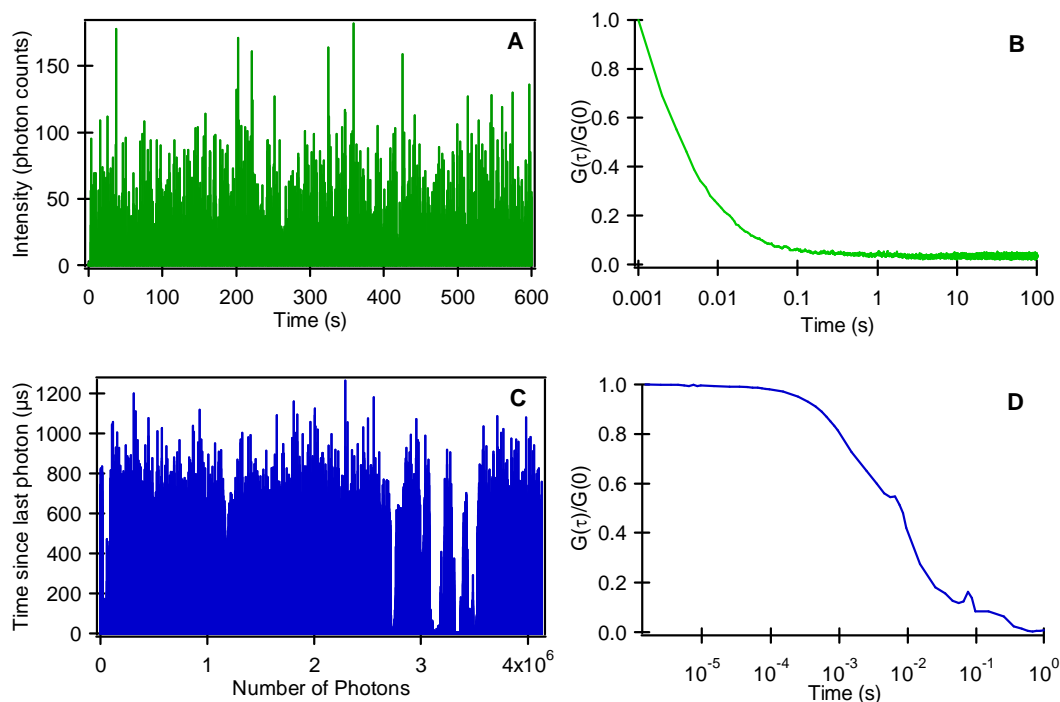
Figure 3.5 Traditional photon intensity time trajectory data compared to time-tagged data and resulting autocorrelations
A) Traditional data is recorded as photon counts per acquisition time with 1 msec time resolution. B) Autocorrelation of freely diffusing DNA data in A. C) Time-tagged data is collected as delay time between photons for each detected photon, and valleys in data indicate a large molecule (vesicle) diffusing through laser beam. Time resolution is 1 μsec. D) Autocorrelation of freely diffusing vesicle data in C.

For experiments performed herein, laser light from an argon ion laser at wavelength 514 nm is directed via mirrors and a fiber optic cable to a confocal microscope with a 100X oil immersion objective (Figure 3.6). The laser is focused into solution, and fluorescence is collected through the objective and directed to the base of the microscope using a long pass filter and a notch filter. Finally, the photons are detected using an avalanche photodiode (APD), which is connected to a counter-timer board. The input from the APD acts as a gating mechanism for the counter-timer board. The timer portion emits pulses at a frequency of 80 MHz, which corresponds to a time interval of 12.5 ns. The counter portion counts the number of pulses from the timer from one photon event to the next, and the number of pulses is

30

converted to a length of time, which then becomes a point in the trajectory. Data is collected using a homemade LabVIEW program and autocorrelated using a homemade Igor routine for Igor Pro.[25]
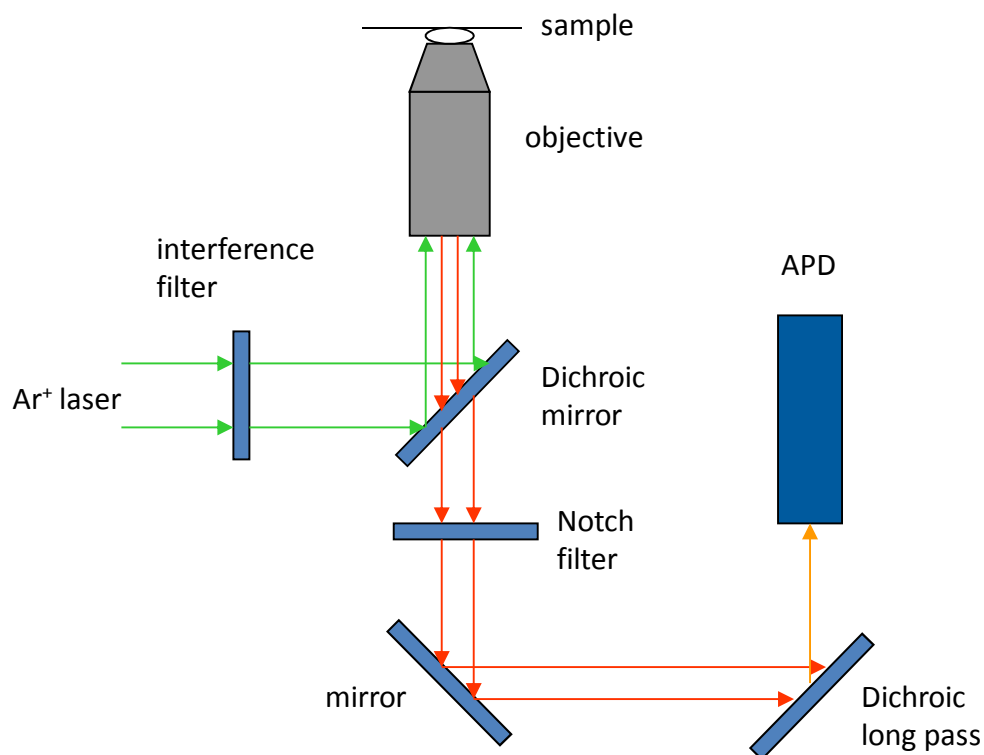
Figure 3.6 Microscope setup for FCS
The laser light is directed through an interference filter and reflected off a dichroic mirror into the objective where it is then focused in the sample solution. The resulting fluorescence is collected through the objective where it then passes through the dichroic mirror, through a notch filter, and then reflected onto the avalanche photodiode (APD).

References

1.   Magde, D.; Webb, W. W.; Elson, E., Thermodynamic fluctuations in a

        reacting system - measurement by fluorescence correlation spectroscopy.

        Phys. Rev. Lett. **1972,** 29, (11), 705-708.

2.   Magde, D.; Elson, E. L.; Webb, W. W., Fluorescence correlation spectroscopy

        2. Experimental realization. *Biopolymers* **1974,** 13, (1), 29-61.

3.   Elson, E. L.; Magde, D., Fluorescence correlation spectroscopy 1. Conceptual

        basis and theory. *Biopolymers* **1974,** 13, (1), 1-27.

4.   Hess, S. T.; Huang, S. H.; Heikal, A. A.; Webb, W. W., Biological and

        chemical applications of fluorescence correlation spectroscopy: A review.

        Biochem. **2002,** 41, (3), 697-705.

5.   Berne, B. J.; Pecora, R., *Dynamic light scattering: With applications to

        chemistry, biology, and physics*. John Wiley & Sons, Inc.: New York, NY,

        1976.

6.   Aragon, S. R.; Pecora, R., Fluorescence correlation spectroscopy as a probe of

        molecular-dynamics. *J. Chem. Phys.* **1976,** 64, (4), 1791-1803.

7.   Eigen, M.; Rigler, R., Sorting single molecules - application to diagnostics

        and evolutionary biotechnology. *Proc. Natl. Acad. Sci. USA* **1994,** 91, (13),

        5740-5747.

8.   Koppel, D. E.; Axelrod, D.; Schlessinger, J.; Elson, E. L.; Webb, W. W.,

        Dynamics of fluorescence marker concentration as a probe of mobility.

        Biophys. J. **1976,** 16, (11), 1315-1329.

9.   Lioi, S. B. W., X.; Islam, M.R.; Danoff, E.J.; English, D.S., Catanionic surfactant vesicles for electrostatic molecular sequestration and encapsulation. *Phys. Chem. Chem. Phys.* **2009,** 11, 9315-9325.

10.   Webb, W. W., Fluorescence correlation spectroscopy: Inception, biophysical experimentations, and prospectus. *Appl. Opt.* **2001,** 40, (24), 3969-3983.

11.   Hess, S. T.; Heikal, A. A.; Webb, W. W., Fluorescence photoconversion kinetics in novel green fluorescent protein pH sensors (pHluorins). *J. Phys. Chem. B* **2004,** 108, (28), 10138-10148.

12.   Lieto, A. M.; Cush, R. C.; Thompson, N. L., Ligand-receptor kinetics measured by total internal reflection with fluorescence correlation spectroscopy. *Biophys. J.* **2003,** 85, (5), 3294-3302.

13.   Petrek, Z.; Schwille, P., Photobleaching in two-photon scanning fluorescence correlation spectroscopy. *Chemphyschem* **2008,** 9, (1), 147-158.

14.   Gould, T. J.; Bewersdorf, J.; Hess, S. T., A quantitative comparison of the photophysical properties of selected quantum dots and organic fluorophores. *Z. Phys. Chem.* **2008,** 222, (5-6), 833-849.

15.   Rochira, J. A.; Gudheti, M. V.; Gould, T. J.; Laughlin, R. R.; Nadeau, J. L.; Hess, S. T., Fluorescence intermittency limits brightness in CdSe/ZnS nanoparticles quantified by fluorescence correlation spectroscopy. *J. Phys. Chem. C* **2007,** 111, (4), 1695-1708.

16.   Haupts, U.; Maiti, S.; Schwille, P.; Webb, W. W., Dynamics of fluorescence fluctuations in green fluorescent protein observed by fluorescence correlation spectroscopy. *Proc. Natl. Acad. Sci. USA* **1998,** 95, (23), 13573-13578.

17.   Heikal, A. A.; Hess, S. T.; Webb, W. W., Multiphoton molecular spectroscopy and excited-state dynamics of enhanced green fluorescent protein (EGFP): Acid-base specificity. *Chem. Phys.* **2001,** 274, (1), 37-55.

18.   Thompson, N. L.; Steele, B. L., Total internal reflection with fluorescence correlation spectroscopy. *Nat. Protoc.* **2007,** 2, (4), 878-890.

19.   Allen, N. W.; Thompson, N. L., Ligand binding by estrogen receptor beta attached to nanospheres measured by fluorescence correlation spectroscopy. *Cytometry A* **2006,** 69A, (6), 524-532.

20.   Larson, D. R.; Gosse, J. A.; Holowka, D. A.; Baird, B. A.; Webb, W. W., Temporally resolved interactions between antigen-stimulated IgE receptors and Lyn kinase on living cells. *J. Cell Biol.* **2005,** 171, (3), 527-536.

21.   Schwille, P.; Korlach, J.; Webb, W. W., Fluorescence correlation spectroscopy with single-molecule sensitivity on cell and model membranes. *Cytometry* **1999,** 36, (3), 176-182.

22.   Rusu, L.; Gambhir, A.; McLaughlin, S.; Radler, J., Fluorescence correlation spectroscopy studies of peptide and protein binding to phospholipid vesicles. *Biophys. J.* **2004,** 87, (2), 1044-1053.

23.   Horton, M. R.; Radler, J.; Gast, A. P., Phase behavior and the partitioning of caveolin-1 scaffolding domain peptides in model lipid bilayers. *J. Colloid Interf. Sci.* **2006,** 304, (1), 67-76.

24.   Eggeling, C.; Berger, S.; Brand, L.; Fries, J. R.; Schaffer, J.; Volkmer, A.; Seidel, C. A. M., Data registration and selective single-molecule analysis

using multi-parameter fluorescence detection. *J. Biotechnol.* **2001,** 86, (3), 163-180.

25. Wang, X. Study of electrostatic interaction between charged surfactant vesicles and ionic molecules by bulk and fluorescence correlation spectroscopy measurements. Ph.D. Dissertation, University of Maryland College Park, College Park, 2007.

Chapter 4: Catanionic Surfactant Vesicles for Electrostatic Molecular Sequestration and Separation

4.1 Introduction

In an effort to quantify interfacial adsorption of DNA at the bilayer exterior, fluorescence correlation spectroscopy (FCS) studies were conducted. Using FCS, the adsorption of a small organic ion, carboxyfluorescein (CF),[1] and a single stranded DNA (ssDNA) molecule were compared in an attempt to compare and contrast the two systems. DNA adsorption is an important topic for transfection applications, which is one of the proposed biotechnological uses for catanionic surfactant vesicles. Catanionic surfactant vesicles have been proposed as a replacement for conventional phospholipid vesicles because of their long term stability. For these studies of DNA binding to surfactant vesicles, FCS offers the advantage of using only small amounts of sample. This is particularly advantageous when working with DNA that has to be isolated and purified from cells, as it would in transfection applications. FCS is a powerful technique for measuring molecular interactions with very low fluorophore concentrations based on the fluorescence intensity fluctuations associated with the diffusion of fluorophores into and out of a laser beam.[2]

4.2   Materials

Amine modified DNA 40 base oligomer for subsequent labeling was ordered from Integrated DNA Technologies. Succinimidyl ester Alexa 555 reactive dye for labeling DNA was ordered from Molecular Probes. Sodium chloride, magnesium chloride, and sodium bicarbonate for fluorescent labeling buffer were purchased from Fisher Scientific. The surfactants CTAT and SDBS were ordered from Aldrich Chemicals and were kept in a desiccator to prevent water absorption. The fluorescent dye rhodamine 6G was purchased from Fluka. G25 illustra MicroSpin columns were purchased from GE Healthcare. Water used in FCS experiments and vesicle preparations was purified using a Millipore water purification system.

4.3   Methods

4.3.1 Vesicle Preparation

Vesicle samples were prepared at a total surfactant concentration of 1% by weight. Vesicle preparations used here were 7:3 CTAT:SDBS by weight, so 0.07 g CTAT and 0.03 g SDBS were weighed out and Millipore water was added to bring the total mass to 10 g. The vesicle solution was stirred for several days to ensure surfactants had dissolved and equilibrium had been reached.

4.3.2 DNA Labeling

Amine modified 40mer DNA from IDT was rehydrated using 10 µL of Millipore purified water. Buffer for labeling reactions was made using 25 mg of sodium bicarbonate dissolved in 1 mL of Millipore purified water. For the labeling reaction, 3 µL of rehydrated amine modified DNA was added to 5 µL of labeling

buffer. The Alexa 555 dye was dissolved using 2 µL of DMSO, then the 8 µL DNA/buffer mixture was added to the dissolved dye, and then the reaction was placed in a 37 °C water bath for three hours. The labeling reaction was taken out of the water bath, 55 µL of labeling buffer was added, and the DNA was separated from the excess dye using a G25 MicroSpin column. The DNA was ethanol precipitated after 20 µL of 1 M NaCl, 2 µL 1 M $MgCl_2$, and 108 µL of Millipore purified water were added. Following ethanol precipitation, the DNA was vacuum dried and rehydrated in Millipore purified water. UV-Vis measurements were done to determine labeling efficiency and DNA concentration following the labeling procedure.

4.3.3 Fluorescence Correlation Spectroscopy

FCS was performed with an instrument described previously[3,4] consisting of an air cooled argon ion laser (532-AP-A01, Melles Griot, Carlsbad, CA), an inverted microscope (Axiovert 200, Carl Zeiss, Göttingen, Germany) and a single photon counting avalanche photodiode (SPCM-AQR-15, Perkin Elmer, Vaudreuil, QC, Canada). The collimated laser beam (λ= 514 nm) was focused into the sample solution approximately 10 µm from the coverslip surface using a 100X, 1.30 N.A. oil immersion objective (Fluar, Carl Zeiss). A nearly diffraction limited spot with a lateral radius of r = 360 nm was achieved. Typical laser power was 5 µW. Fluorescence was collected through the objective and filtered through a holographic notch filter (λ= 514.4 nm, Kaiser Optical, Ann Arbor, MI) to remove scattered excitation light. Collection optics consisted of a pair of achromatic doublets placed after the primary image plane and were used to match the size of the colleted fluorescence spot with the 180 µm diameter area of the APD. The output of the APD

was fed to a counter timer board (PCI-6602, National Instruments, Austin TX) operating in time-tagged photon counting mode using home written software in LabVIEW (National Instruments, Austin, TX.).

The adsorption of 40mer ssDNA to CTAT-rich vesicles was studied using preformed vesicles, followed by DNA addition and overnight sample equilibration before performing FCS experiments. Vesicles were prepared in the ratio of 7:3 CTAT:SDBS, with a total of 1% surfactant by weight and then diluted for each sample prepared. A constant concentration of 10 nM 40mer ssDNA was used with varying surfactant concentrations. The DNA diffusion coefficient was determined by performing FCS on a 10 nM solution of 40mer ssDNA and fitting the autocorrelation curve to Equation 4.3. Equation 4.4 was used to fit the solutions containing both vesicles and DNA. When fitting these autocorrelation curves, the vesicle diffusion coefficient was not held constant, but the diffusion coefficient for the DNA was held constant. The FCS DNA binding experiments were performed in triplicate, and the fraction of DNA bound to vesicles, f, was determined from fitting the autocorrelation curves to equation 4.4. All three values for the fraction bound at each surfactant concentration were averaged, and one standard deviation around the average was also calculated.

Finally, the fraction of DNA bound to vesicles, f, was plotted versus surfactant concentration for each mixture of vesicles and DNA. Error bars were constructed that were one standard deviation around the average of all f values for a certain surfactant concentration. An adsorption isotherm was constructed using this data and fit to the following equation:

$$f = \frac{K \times C}{1 + (K \times C)} \tag{4.1}$$

where C is the surfactant concentration and K is the binding constant.

4.4 Results and Discussion

FCS was implemented to measure the fraction of adsorbed dye molecules as a function of total surfactant concentration, and FCS was performed with an instrument described previously.[3,4] The fluorescence intensity fluctuations were recorded from solutions of dye molecules (10 nM) while varying the concentration of vesicle-forming surfactant mixtures.[1] The fluctuations were processed by standard autocorrelation analysis according to the following equation (described in more detail in chapter 3):

$$G(\tau) = \frac{\langle \delta F(t) \delta F(t+\tau) \rangle}{\langle F(t) \rangle^2}. \tag{4.2}$$

Figure 4.1A shows fluorescence fluctuation autocorrelation decays acquired for CF in water at three different concentrations. The decays are fit with the functional form describing a single fluorescent species freely diffusing through an ellipsoidal 3D-gaussian observation volume:

$$G(\tau) = C * \left(\frac{1}{1 + \frac{\tau}{\tau_D}} \right) * \left(\frac{1}{1 + \omega^2 \frac{\tau}{\tau_D}} \right)^{\frac{1}{2}} \tag{4.3}$$

where C is inversely proportional to the average number of molecules in the observation volume, τ_D is the characteristic diffusion time related to the lateral beam dimension r_0 and the lateral diffusion constant D by $\tau_D = r_0^2/4D$. The quantity ω^2 is a factor proportional to the ratio of the radial and axial axes of the

three dimensional observation volume.[5,6] The best-fit parameters for the three

curves in Figure 4.1A are consistent with expectations, yielding amplitudes that

are inversely proportional to concentration and a diffusion coefficient,

$D = 1.5 \times 10^{-6}$ cm^{2}s^{-1}, consitent with previously reported values.[7]
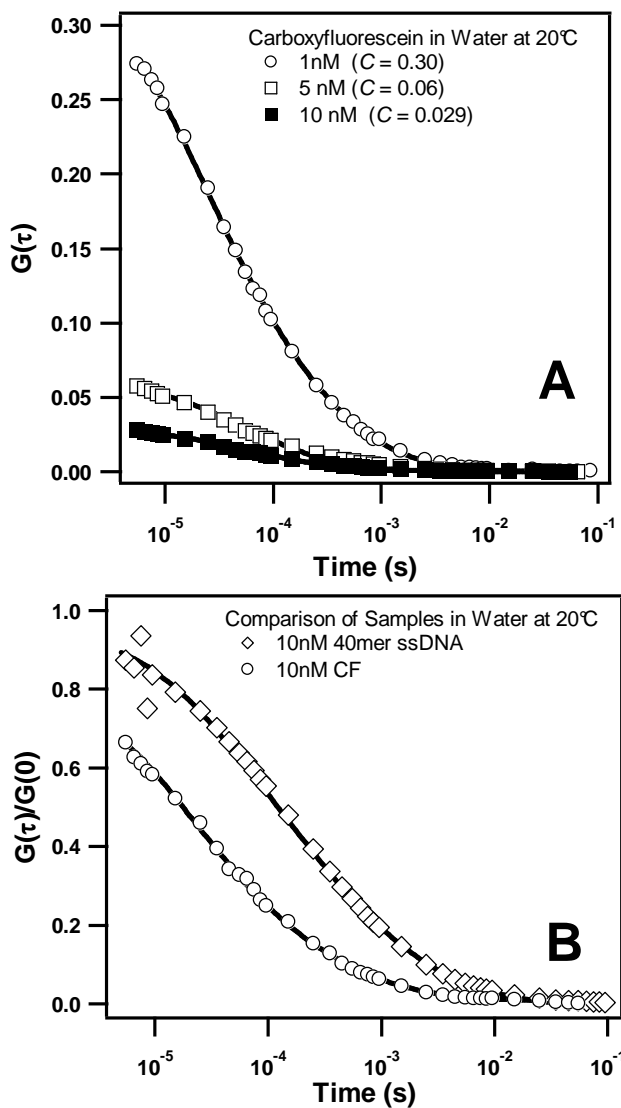
Figure 4.1 FCS results for dyes and DNA in water
A) Autocorrelation decays for 1 nM, 5 nM, and 10 nM carboxyfluorescein samples.
B) Autocorrelation decays for 10 nM CF and 10 nM 40mer ssDNA.

Figure 4.1B shows a comparison of autocorrelation decays acquired for 10

nM solutions of the dye carboxyfluorescein (CF) and a 40 base dye-labeled

ssDNA sequence referred to as the 40mer. To perform FCS, the 40mer was covalently labeled with Alexa555. For the 40mer sequence, $D = 7.5 \times 10^{-7}$ cm^{2}s^{-1}, which is in good agreement with literature values of similar sized ssDNA.[8] The clear distinction between the two traces in Figure 4.1B illustrates the ability of the FCS technique to distinguish different species in solution, and this has proven to be a powerful technique for studying the interaction of biological molecules with vesicles and beads.[9,10] We have utilized this ability to investigate binding of dye and DNA molecules to oppositely charged surfactant vesicles.

The adsorption of probe molecules to the exterior of surfactant vesicles was studied by adding pre-formed vesicles to dye solutions. In all cases the dye concentration was 10 nM with varying surfactant concentrations. These samples were studied with FCS and the autocorrelation decays were fit to a two component equation:

$$G(\tau) = f * \left(\frac{1}{1+\frac{\tau}{\tau_v}}\right) * \left(\frac{1}{1+\omega^2\frac{\tau}{\tau_v}}\right)^{\frac{1}{2}} + (1-f) * \left(\frac{1}{1+\frac{\tau}{\tau_p}}\right) * \left(\frac{1}{1+\omega^2\frac{\tau}{\tau_p}}\right)^{\frac{1}{2}} \quad (4.4)$$

where f is the fraction of probe molecule (dye) that is bound to vesicles. The diffusion times for vesicles and dye molecules are τ_v and τ_p, respectively. Diffusion times for probe molecules were determined from autocorrelation decays obtained in the absence of vesicles. Separate experiments were conducted in which vesicle diffusion times were determined independently using the autocorrelation decay of vesicles doped with a low concentration (0.1 µM) of the lipophilic dye DiIC$_{18}$. The diffusion times for DiIC$_{18}$ doped vesicles yield values of D that agree well with those

calculated for vesicles with radii of 70 nm at 293 K using the Stokes-Einstein equation.

Figure 4.2A shows a series of autocorrelation decays from mixtures containing the anionic dye CF with increasing amounts of equilibrated CTAT-rich solutions. In this example the decay grows longer as the surfactant concentration increases. The increase in autocorrelation decay time is due to electrostatic adsorption of the dye to surfactant aggregates rich in CTA^+. These aggregates are almost certainly vesicles, since the decay time, τ_D, is consistent with 150 nm diameter vesicles. These values are consistent with our previous studies of dye adsorption using both DLS and small angle light scattering.[11] Control experiments in which the SDBS-rich mixture is added show no increase in the decay lifetime. Additionally, control experiments with only CTAT added show an increase in decay time consistent with the formation of micelles, not vesicles.

A sudden increase in the decay time occurs in Figure 4.2A when the total surfactant concentration goes above 40 µM. Below this point the autocorrelation decay is consistent with free, unadsorbed dye. Below 40 µM there is no measurable association with vesicles even though this concentration is well above the cac. The data in Figure 4.2A was fit to equation 4.4 using two diffusion coefficients consistent with free dye (10^{-6} cm^2s^{-1}) and vesicles (10^{-9} cm^2s^{-1}). From the fit we obtained a value of f for each mixture and these values are plotted in Figure 4.2B. Figure 4.2B does not follow a simple adsorption isotherm but instead shows a slight lag phase followed by a Langmuir-like region and binding saturation at 200 µM, which is well above the cac. In these experiments, the dye solution was added to pre-equilibrated surfactant

mixtures and therefore the rise in Panel 4.2B reflects interaction between anionic CF and the CTAT-rich vesicle exterior.
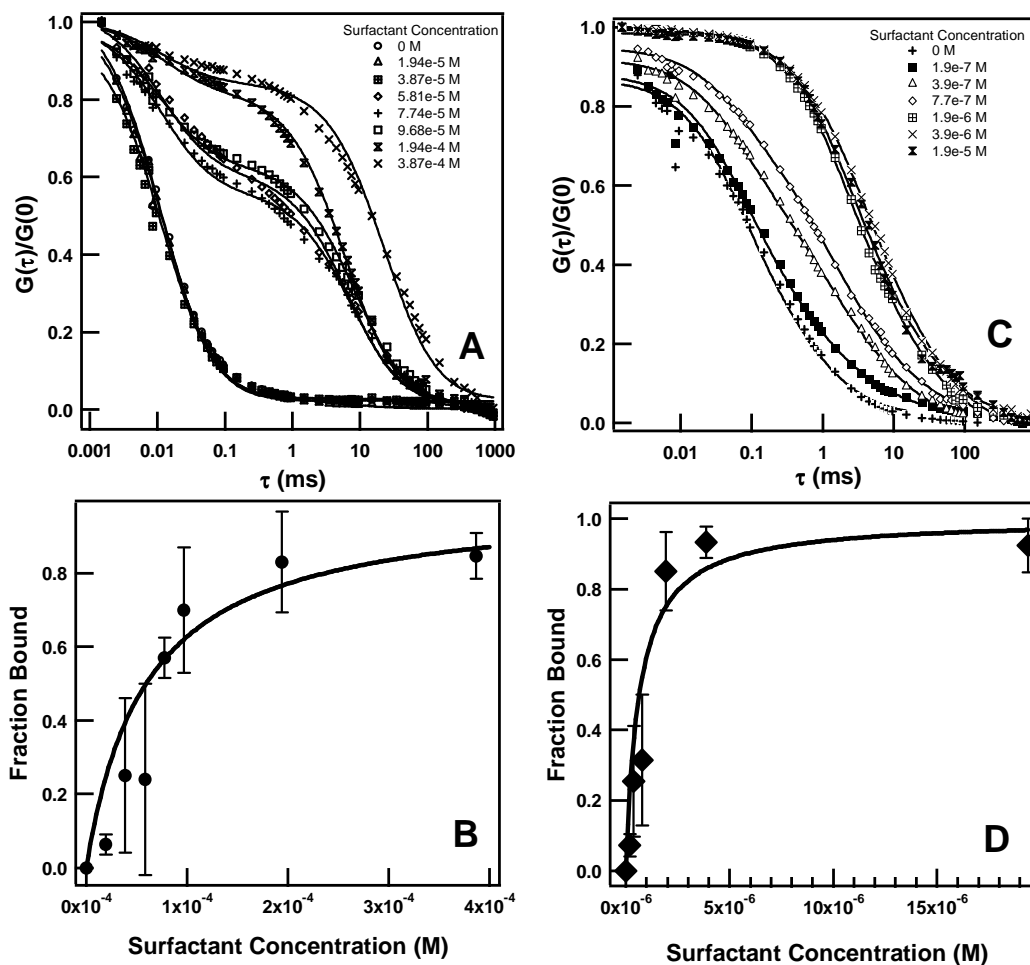
Figure 4.2 Raw data and isotherms for CTAT-rich vesicles with carboxyfluorescein and DNA
A) Autocorrelation curves for 10nM carboxyfluorescein with varying concentrations of surfactant. B) Binding isotherm for carboxyfluorescein and CTAT-rich vesicles. C) Autocorrelation curves for 10nM 40mer ssDNA with varying concentrations of surfactant. D) Binding isotherm for 40mer ssDNA and CTAT-rich vesicles.

Figure 4.2C is analogous to Figure 4.2A, but the fluorescent probe is a 40mer ssDNA labeled with Alexa 555. The results from FCS studies using the dye labeled DNA differ significantly from those of CF in several ways. Most notable is the much lower saturation concentration of 1.9 µM in Panel 4.2D. DNA binding is clearly facilitated by the flexibility and high charge density, which enables the DNA

phosphate groups to pair with multiple CTA$^+$ monomers in the vesicle bilayer, and this is consistent with the lower saturation point.

There is also a notable difference between the autocorrelation decays at saturation for the two systems, as seen in Panels A and C of Figure 4.2. The autocorrelation decay obtained from CF at 3.9 x 10^{-4} M is substantially slower than that of the 40mer at 1.9 x 10^{-6} M, indicating that the CF probe is bound to a larger aggregate. The vesicle radius measured by FCS with CF is approximately five times greater than that measured by DLS in 1% w/w solutions.[11] This observation is not inconsistent with previous measurements using DLS by McKelvey et al. who report dramatic increases in CTAT-rich vesicle radii at high dilution.[12] The shorter decay times observed at saturation for the 40mer studies correspond to a vesicle radius of 75 nm, which is consistent with DLS measurements at higher concentrations. These results strongly suggest that the presence of DNA appears to stabilize a higher curvature as the cac is approached when compared to CF or neat vesicles. Previous reports have shown that polyelectrolytes can affect vesicle morphology.[13]

The saturation point in Figure 4.2D corresponds to a DNA mole fraction of X_{DNA}= [DNA]/([DNA] + S) =0.005 and a nucleotide mole fraction of X_{nt}=0.21. Hence DNA forms a significant component of the aggregates detected by FCS at the saturation point. The concentration of vesicles at the DNA saturation point can be estimated at 6.5 x 10^{-12} M by assuming an average vesicle radius of 75 nm and an average surfactant head group area of 0.48 nm^2.[14] This is an upper limit that assumes all surfactant molecules are aggregated and gives an estimated DNA 40mer/vesicle ratio of 1.5 x 10^3. While this number is only a rough estimate, it demonstrates that

each vesicle consists of a significant amount of DNA, presumably adsorbed to the bilayer exterior.

Other groups have observed significant morphological changes induced by polymer interactions with vesicles. For instance, Lee and coworkers observed morphological changes induced by hydrophobic ends on modified chitosan, a naturally occurring polysaccharide.[15] In their experiments, modified chitosan associates with the vesicle bilayer through hydrophobic insertion, and at low concentrations the vesicle size decreases by about 50%. Upon further addition of polymer, co-existence of unilamellar and bilamellar vesicles is observed. In a separate study, Regev and co-workers used cryogenic transmission electron microscopy to record morphological changes induced by polyelectrolytes electrostatically adsorbed to the exterior of negatively charged vesicles that include formation of disk-like aggregates and "faceted" vesicles.[13] These transitions were observed at relatively low polymer concentrations. To characterize the relative amount of polyelectrolyte present in the solution, they calculated a charge mole fraction, which is the fraction of polymer charge relative to the excess charge of the surfactant system. We used this value to characterize our systems at saturation:

$$F_- = \frac{C_-}{C_- + (C_{CTAT} - C_{SDBS})}$$
(4.5)

where C_- is the total molar concentration of adsorbate charge, i.e. concentration of nucleotides. The value at adsorption saturation for DNA shows that 75% of the excess surfactant in the mixture is balanced by phosphate groups of the DNA adsorbate. This remarkably high degree of charge neutralization would certainly have an effect on the bilayer curvature based on the arguments given for spontaneous

46

curvature in Chapter 1,[16] and one would expect that charge neutralization would lower the curvature. However, it appears this is not the case given the smaller vesicle size measured with bound DNA versus bound CF.

Figure 4.3 shows the DNA adsorption isotherm superimposed with surface tension data which closely matches previous measurements.[17] The surface tension data indicates a cac of 2.6 µM in good agreement with previous measurements.[18] The fact that the saturation point for the 40mer matches well with measured values of the cac is significant because it suggests that DNA may have a stabilizing effect on vesicle formation. The formation of single DNA-surfactant globules with cationic surfactants in dilute solutions has been well documented.[19] Such aggregates have a distinctly smaller hydrodynamic radius than that measured above in Figure 4.2B. In fact, these globules are smaller than the free DNA itself. Furthermore, these aggregates are unstable in the presence of co-solutes including anionic surfactants.[20] Many studies have appeared in the literature documenting the interaction of DNA with positively-charged catanionic vesicles.[19, 21-26] Mel'nikov et al showed that large Coliphage T4 DNA molecules (10^8 D) remain in an extended conformation in the presence of sodium octyl sulfate-rich (SOS-rich) catanionic vesicles formed from SOS and CTAB. They noted that when CTAB was the minor component, the DNA conformation was not measurably affected. This result suggested that CTAB, as the minor component, was sufficiently stable in the vesicle bilayer that it did not exist in solution at a high enough concentration to cause DNA compaction: even at CTAB concentrations as high as 29 mM there was no compaction observed. In CTAB-rich

mixtures they observed compaction and in solutions with a 1.15:1.00 molar ratio of CTAB-to-SOS they found the DNA adsorbed to the vesicle surface.[19]
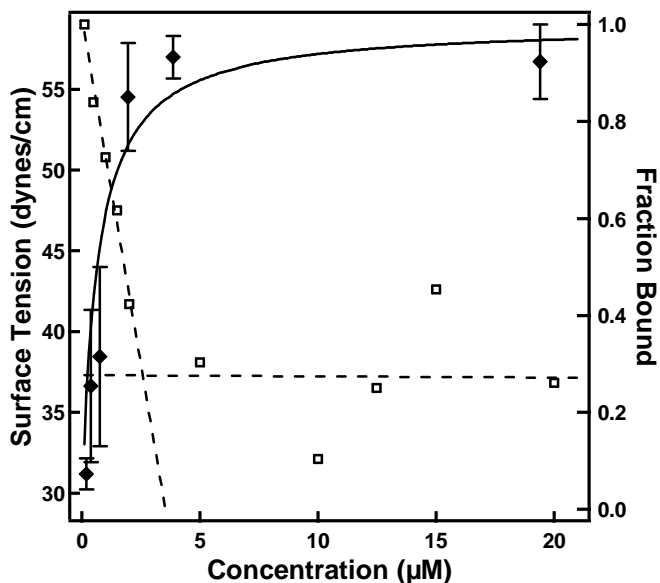
Figure 4.3 Surface tension measurements of 7:3 CTAT:SDBS surfactant mixture and isotherm for ssDNA 40mer
The 7:3 CTAT:SDBS surfactant data is denoted by (□) and isotherm for ssDNA data denoted by (♦). The dashed lines are linear fits of the two portions of the surface tension data. The lines intersect at 2.6 μM surfactant. The isotherm data are from Figure 4.2 and the solid line is simply meant to guide the eye.

The data from CTAT-rich samples presented in Figure 4.2 was collected at surfactant concentrations of 10^3-10^4 lower than those presented by Mel'nikov. Additionally, the DNA used in our experiments are small single stranded oligomers and it is unlikely that large globular aggregates would form. Hence we believe that the saturation point in Figure 4.2D corresponds to vesicles coated with DNA. As pointed out above, this observation suggests that there is a relatively abundant number of vesicles present at surfactant concentrations slightly below the cac we measured and those reported previously.[18] This is unexpected since vesicles should be the minor component just above the cac and absent below the cac, however the

consistency of the autocorrelation decays at $S \geq 1.94$ µM implies that vesicles are present and stable below the cac when DNA is present. While we cannot state with absolute certainty that the structures are unilamellar vesicles, the data strongly supports the fact that large aggregates exist. Direct imaging by methods such as cryo-TEM would likely yield little definitive evidence given the very low sample concentrations. Additional evidence that we observe vesicles comes from the fact that our results mirror those reported recently in which the lowering of the cac and formation of vesicles by dodecyltriethylammonium bromide (DEAB) in the presence of DNA was reported by Guo and coworkers.[27]

The findings in this section show that FCS provides a convenient method for monitoring the electrostatic binding strength of a solute to the exterior interface of the catanionic vesicle bilayer. Using this method we have monitored electrostatic adsorption of probe molecules to vesicle exteriors and this has allowed us to monitor interactions down to concentrations where vesicles begin to become unstable.

4.5   Conclusions

Catanionic surfactant vesicles display useful properties in sequestration of oppositely charged solutes, whether they are small organic molecules or polyelectrolytes such as DNA. These systems have been utilized as separations media, and due to their stability and strong electrostatic interactions, catanionic surfactant vesicles are promising in the areas of drug delivery and gene therapy, especially since DNA binds so strongly to CTAT-rich vesicles. Advantages of these systems include low cost and ease of preparation, and long term stability and

robustness with respect to pH and ionic strength. Challenges for biotechnological applications include development of formulations that utilize biologically-degradable or non-toxic components. It is interesting to note that regular solution theory predicts a small amount of CTAT in the bilayer at low surfactant concentrations; however, if this was the case, it is unlikely that DNA would bind so strongly. Regular solution theory is perhaps only applicable at higher surfactant concentrations and not relevant when DNA is present in solution. Future studies with surfactant vesicles will focus on the toxicity and delivery capabilities of these vesicles. It is likely that very low surfactant concentrations will not cause harm to cells, thus DNA stabilized vesicles could be used in biological study. Additionally, the long-term stablility and slow release properties of catanionic vesicles may make them good candidates for time-release applications in chemotherapy. For instance, the enhanced permeability and retention observed for tumor tissue with respect to liposome-sized particles suggests that drug bearing catanionic vesicles that find their way, or are targeted to, tumor vasculature will be taken up and retained by the tumor tissue.[28] This could shorten the time required between chemotherapy treatments.

References

1.   Wang, X. Study of electrostatic interaction between charged surfactant vesicles and ionic molecules by bulk and fluorescence correlation spectroscopy measurements. Ph.D. Dissertation, University of Maryland College Park, College Park, 2007.

2.   Magde, D.; Elson, E. L.; Webb, W. W., Fluorescence correlation spectroscopy. II. Experimental realization. *Biopolymers* **1974,** 13, (1), 29-61.

3.   Morgan, M. A.; Okamoto, K.; Kahn, J. D.; English, D. S., Single-molecule spectroscopic determination of lac repressor-DNA loop conformation. *Biophys. J.* **2005,** 89, (4), 2588-2596.

4.   Pons, T.; Medintz, I. L.; Wang, X.; English, D. S.; Mattoussi, H., Solution-phase single quantum dot fluorescence resonance energy transfer. *J. Am. Chem. Soc.* **2006,** 128, (47), 15324-15331.

5.   Hess, S. T.; Webb, W. W., Focal volume optics and experimental artifacts in confocal fluorescence correlation spectroscopy. *Biophys. J.* **2002,** 83, (4), 2300-2317.

6.   Thompson, N. L., In *Topics in fluorescence spectroscopy*, Lakowicz, J. R., Ed. Plenum Press: New York, 1991; pp 337-378.

7.   Gregoriadis, G.; Florence, A. T., Liposomes in drug delivery - Clinical, diagnostic and ophthalmic potential. *Drugs* **1993,** 45, (1), 15-28.

8.   Moghimi, S. M.; Hunter, A. C.; Murray, J. C., Nanomedicine: Current status and future prospects. *FASEB J.* **2005,** 19, (3), 311-330.

9.   Allen, N. W.; Thompson, N. L., Ligand binding by estrogen receptor beta attached to nanospheres measured by fluorescence correlation spectroscopy. *Cytometry A* **2006,** 69A, (6), 524-532.

10.   Rusu, L.; Gambhir, A.; McLaughlin, S.; Radler, J., Fluorescence correlation spectroscopy studies of peptide and protein binding to phospholipid vesicles. *Biophys. J.* **2004,** 87, (2), 1044-1053.

11.   Danoff, E. J.; Wang, X.; Tung, S.-H.; Sinkov, N. A.; Kemme, A. M.; Raghavan, S. R.; English, D. S., Surfactant vesicles for high-efficiency capture and separation of charged organic solutes. *Langmuir* **2007,** 23, 8965-8971.

12.   McKelvey, C. A.; Kaler, E. W.; Zasadzinski, J. A.; Coldren, B.; Jung, H. T., Templating hollow polymeric spheres from catanionic equilibrium vesicles: Synthesis and characterization. *Langmuir* **2000,** 16, (22), 8285-8290.

13.   Regev, O.; Marques, E. F.; Khan, A., Polymer-induced structural effects on catanionic vesicles: Formation of faceted vesicles, disks, and cross-links. *Langmuir* **1999,** 15, (2), 642-645.

14.   Walker, S. A.; Zasadzinski, J. A., Electrostatic control of spontaneous vesicle aggregation. *Langmuir* **1997,** 13, (19), 5076-5081.

15.   Lee, J. H.; Agarwal, V.; Bose, A.; Payne, G. F.; Raghavan, S. R., Transition from unilamellar to bilamellar vesicles induced by an amphiphilic biopolymer. *Phys. Rev. Lett.* **2006,** 96, (4), 048102.

16.   Safran, S. A.; Pincus, P.; Andelman, D., Theory of spontaneous vesicle formation in surfactant mixtures. *Science* **1990,** 248, (4953), 354-356.

17.   Kaler, E. W.; Herrington, K. L.; Miller, D. D.; Zasadzinski, J. A., Phase behavior of aqueous mixtures of anionic and cationic surfactants along a dilution path. In *Structure and dynamics of strongly interacting colloids and supramolecular aggregates in solution*, Chen, S.-H.; Huang, J. S.; Tartaglia, P., Eds. Kluwer Academic Publishers: Dordrecht, 1992; Vol. 369. pp 571-577.

18.   Chiruvolu, S.; Israelachvili, J. N.; Naranjo, E.; Xu, Z.; Zasadzinski, J. A.; Kaler, E. W.; Herrington, K. L., Measurement of forces between spontaneous vesicle-forming bilayers. *Langmuir* **1995,** 11, (11), 4256-4266.

19.   Mel'nikov, S. M.; Dias, R.; Mel'nikova, Y. S.; Marques, E. F.; Miguel, M. G.; Lindman, B., DNA conformational dynamics in the presence of catanionic mixtures. *FEBS Lett.* **1999,** 453, (1,2), 113-118.

20.   Dias, R. S.; Lindman, B.; Miguel, M. G., Compaction and decompaction of DNA in the presence of catanionic amphiphile mixtures. *J. Phys. Chem. B* **2002,** 106, (48), 12608-12612.

21.   Bonincontro, A.; Falivene, M.; La Mesa, C.; Risuleo, G.; Pena, M. R., Dynamics of DNA adsorption on and release from SDS-DDAB cat-anionic vesicles: A multitechnique study. *Langmuir* **2008,** 24, (5), 1973-1978.

22.   Bonincontro, A.; La Mesa, C.; Proietti, C.; Risuleo, G., A biophysical investigation on the binding and controlled DNA release in a cetyltrimethylammonium bromide-sodium octyl sulfate cat-anionic vesicle system. *Biomacromolecules* **2007,** 8, (6), 1824-1829.

23.   Dias, R. S.; Lindman, B.; Miguel, M. G., DNA interaction with catanionic vesicles. *J. Phys. Chem. B* **2002,** 106, (48), 12600-12607.

24. Dias, R. S.; Pais, A.; Miguel, M. G.; Lindman, B., DNA and surfactants in bulk and at interfaces. *Colloids Surf., A* **2004,** 250, (1-3), 115-131.

25. Rosa, M.; Miguel, M. D.; Lindman, B., DNA encapsulation by biocompatible catanionic vesicles. *J. Colloid Interf. Sci.* **2007,** 312, (1), 87-97.

26. Rosa, M.; Moran, M. D.; Miguel, M. D.; Lindman, B., The association of DNA and stable catanionic amino acid-based vesicles. *Colloids Surf., A* **2007,** 301, (1-3), 361-375.

27. Guo, X.; Li, H.; Zhang, F. M.; Zheng, S. Y.; Guo, R., Aggregation of single-chained cationic surfactant molecules into vesicles induced by oligonucleotide. *J. Colloid Interf. Sci.* **2008,** 324, (1-2), 185-191.

28. Maeda, H.; Greish, K.; Fang, J., The EPR effect and polymeric drugs: A paradigm shift for cancer chemotherapy in the 21st century. In *Advances in polymer science*, Springer-Verlag Berlin: Berlin, 2006; Vol. 193, pp 103-121.

Chapter 5: Fluorescence Correlation Spectroscopy Studies of Electrostatic Adsorption of Small DNA Molecules to Catanionic Surfactant Vesicles

5.1 *Introduction*

In this chapter the adsorption of a short piece of single stranded DNA, only five bases long, is compared with the 40 base long ssDNA and the small molecule organic dye carboxyfluorescein (CF). The 40mer ssDNA is also compared to double stranded 40mer DNA. In addition, salt studies were done to determine how the adsorption of cargo molecules to the exterior of the vesicle would be affected by physiological salt concentrations and a different counterion. These surfactant vesicles have been shown to have potential in both drug delivery and gene therapy, thus it is important that the adsorption of the cargo molecule be able to withstand those salt concentrations.

5.2 *Materials*

Amine modified DNA 5 base oligomer for subsequent labeling and unmodified 40 base DNA was ordered from Integrated DNA Technologies. Succinimidyl ester Alexa 555 reactive dye for labeling DNA was ordered from Molecular Probes. Sodium chloride, magnesium chloride, and sodium bicarbonate for fluorescent labeling buffer were purchased from Fisher Scientific. The surfactants CTAT and SDBS were ordered from Aldrich Chemicals and were kept in a desiccator to prevent water absorption. The fluorescent dye rhodamine 6G was purchased from

Fluka. G25 illustra MicroSpin columns were purchased from GE Healthcare. Water used in FCS experiments and vesicle preparations was purified using a Millipore water purification system.

5.3   *Methods*

5.3.1 Vesicle Preparation

Vesicle samples were prepared at a total surfactant concentration of 1% by weight. Vesicle preparations used here were 7:3 CTAT:SDBS by weight and 6.5:3.5 CTAB:SDBS by weight. For the 7:3 CTAT:SDBS vesicles, 0.07 g CTAT and 0.03 g SDBS were weighed out and Millipore water was added to bring the total mass to 10 g. For the 6.5:3.5 CTAB:SDBS vesicles, 0.065 g CTAB and 0.035 g SDBS were weighed out and Millipore water was added to bring the total mass to 10 g. Vesicle solutions were stirred for several days to ensure surfactants had dissolved and equilibrium had been reached.

5.3.2 DNA Labeling

Amine modified 5mer DNA from IDT was rehydrated using 10 µL of Millipore purified water. Buffer for labeling reactions was made using 25 mg of sodium bicarbonate dissolved in 1 mL of Millipore purified water. For the labeling reaction, 3 µL of rehydrated amine modified DNA was added to 5 µL of labeling buffer. The Alexa 555 dye was dissolved using 2 µL of DMSO, then the 8 µL DNA/buffer mixture was added to the dissolved dye, and then the reaction was placed in a 37 °C water bath for three hours. The labeling reaction was taken out of the

water bath, and 55 µL of labeling buffer were added, and the DNA was separated from the excess dye using a G25 MicroSpin column. The DNA was ethanol precipitated after 20 µL of 1 M NaCl, 2 µL 1 M MgCl$_2$, and 108 µL of Millipore purified water were added. Following ethanol precipitation, the DNA was dried and rehydrated in Millipore purified water. UV-Vis measurements were done to determine labeling efficiency and DNA concentration following the labeling procedure.

5.3.3 Fluorescence Correlation Spectroscopy

FCS was performed with an instrument described previously[1,2] consisting of an air cooled argon ion laser (532-AP-A01, Melles Griot, Carlsbad, CA), an inverted microscope (Axiovert 200, Carl Zeiss, Göttingen, Germany) and a single photon counting avalanche photodiode (SPCM-AQR-15, Perkin Elmer, Vaudreuil, QC, Canada). The collimated laser beam (λ=514 nm) was focused into the sample solution approximately 10 µm from the coverslip surface using a 100X, 1.30 N.A. oil immersion objective (Fluar, Carl Zeiss). A nearly diffraction limited spot with a lateral radius of r=360 nm was achieved. Typical laser power was 5 µW. Fluorescence was collected through the objective and filtered (holographic notch filter λ=514.4 nm, Kaiser Optical, Ann Arbor, MI) to remove scattered excitation light. Collection optics consisted of a pair of achromatic doublets placed after the primary image plane and were used to match the size of the colleted fluorescence spot with the 180 µm diameter area of the APD. The output of the APD was fed to a counter timer board (PCI-6602, National Instruments, Austin TX) operating in time-tagged photon counting mode using home written software in LabVIEW (National

Instruments, Austin, TX.). In time-tagged mode, each detected photon is assigned a number corresponding to the elapsed time from the previous detection event. These "time-tags" are then used to reconstruct the photon intensity transient or autocorrelation curve. Temporal resolution for timed tagged data is limited by the dead-time of the APD (50 ns) and the on-board clock of the counter/timer board (80 MHz). The time tagged data was autocorrelated off-line using routines written with Igor Pro 5.0 (Wavemetrics, Portland, OR) according to the following equation:[3]

$$G(\tau) = \frac{\langle \delta F(t) \delta F(t+\tau) \rangle}{\langle F(t) \rangle^2}. \tag{5.1}$$

Autocorrelation curves were then fit with either a one component or two component autocorrelation equation for diffusing molecules. Single stranded DNA autocorrelations were fit to the following single component equation:

$$G(\tau) = C * \left(\frac{1}{1 + \frac{\tau}{\tau_D}} \right) * \left(\frac{1}{1 + \omega^2 \frac{\tau}{\tau_D}} \right)^{\frac{1}{2}} \tag{5.2}$$

where C is inversely proportional to the average number of molecules in the observation volume, τ_D is the characteristic diffusion time ($\tau_D = \frac{r^2}{4D}$ where D is the diffusion coefficient) and ω^2 is a factor proportional to the ratio of the radial and axial axes of the three dimensional observation volume.[3,4]

The adsorption of ssDNA or dsDNA to CTAT-rich vesicles was studied using preformed vesicles, followed by DNA addition and overnight sample equilibration before performing FCS experiments. Vesicles were prepared in the ratio of 7:3 CTAT:SDBS, with a total of 1% surfactant by weight and then diluted for each sample prepared. A constant concentration of 10 nM DNA was used with varying

surfactant concentrations. The autocorrelation curves from these studies were fit to a two component autocorrelation equation:

$$G(\tau) = f * \left(\frac{1}{1+\frac{\tau}{\tau_v}}\right) * \left(\frac{1}{1+\omega^2 \frac{\tau}{\tau_v}}\right)^{\frac{1}{2}} + (1-f) * \left(\frac{1}{1+\frac{\tau}{\tau_p}}\right) * \left(\frac{1}{1+\omega^2 \frac{\tau}{\tau_p}}\right)^{\frac{1}{2}} \quad (5.3)$$

where f is the fraction of probe molecule (dye) that is bound to vesicles, and τ_v and τ_p are the diffusion times for vesicles and DNA molecules, respectively. The DNA diffusion coefficient was determined by performing FCS on a 10 nM solution of each DNA sample and fitting the autocorrelation curve to equation 5.2, and DNA diffusion coefficients compare well with literature values.[5] When fitting the vesicle and DNA solutions using equation 5.3, the vesicle diffusion coefficient was constrained to values on the order of 8×10^{-9} cm^2/s to 3×10^{-8} cm^2/s, but the diffusion coefficient for the DNA was held constant. Vesicle diffusion times were determined using vesicles doped with a low concentration (0.1 μM) of the lipophilic dye DiIC$_{18}$ (see Chapter 4). The FCS DNA binding experiments were performed in triplicate, and the fraction of DNA bound to vesicles, f, was determined from fitting the autocorrelation curves to equation 5.3. All three values for the fraction bound at each surfactant concentration were averaged, and one standard deviation around the average was also calculated.

Finally, the fraction of DNA bound to vesicles, f, was plotted versus surfactant concentration for each mixture of vesicles and DNA. Error bars were constructed that were one standard deviation around the average of all f values for a certain surfactant concentration. An adsorption isotherm was constructed using this data and fit to the following equation:

$$f = \frac{K \times [CTA^+]_{excess}}{1 + (K \times [CTA^+]_{excess})} \tag{5.4}$$

where $[CTA^+]_{excess}$ is the concentration of excess CTAT given by $[CTA^+]_{excess} = [CTAT] - [SDBS]$ and K is the adsorption constant.

5.4 *Results and Discussion*

The spontaneous formation of charged unilamellar vesicles in CTAT/SDBS mixtures is well documented.[6,7] For CTAT/SDBS and other catanionic systems, spontaneous vesicle formation is only observed when one of the surfactants is in stoichiometric excess. Because the excess surfactant is soluble in the vesicle bilayer, these vesicles always carry a net charge. Figure 5.1 is a schematic depiction illustrating how the vesicle bilayer is formed from a mixture of ion-paired surfactants interspersed by monomers of the excess surfactant. The spontaneous curvature necessary to form vesicles is believed to stem from nonideal mixing which results in the majority of the excess surfactant residing in the exterior leaflet. The excess unpaired surfactant in the outer leaflet leads to spontaneous curvature by increasing the average head group separation in the outer leaflet and also imparts a high surface charge to the vesicle.[8]

The unpaired surfactants in the external leaflet also provide electrostatic adsorption sites for counterions in solution. It has been shown previously that these sites can be used to attain relatively high loading of charged organic ions when the cargo molecule is oppositely charged from the bilayer,[9,10] and recently it was demonstrated that FCS can be used to measure adsorption isotherms for small

molecules and a ssDNA molecule adsorbed to CTAT-rich catanionic vesicles. Using FCS the adsorption of probe molecules was followed at concentrations as low as the critical aggregation concentration (cac) where vesicles are just beginning to form.[11]
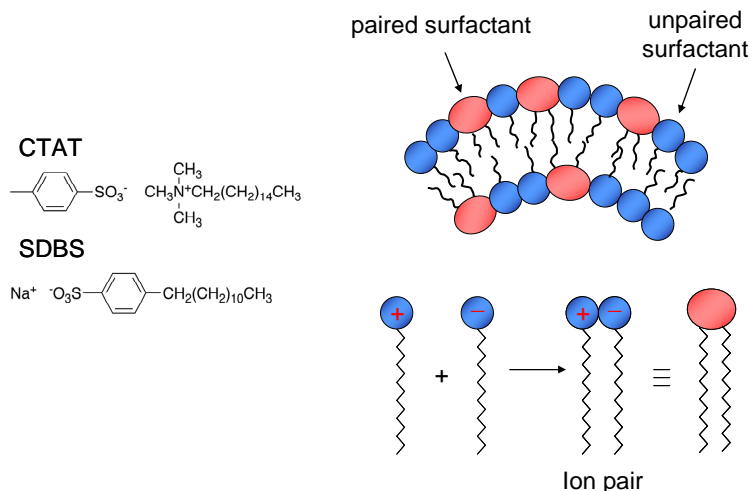
Figure 5.1 Bilayer composition and electrostatic binding

As described in the experimental section, adsorption isotherms can be constructed by measuring the fraction of the fluorescent probe molecule that is adsorbed at the vesicle interface as a function of surfactant concentration. Figure 5.2 shows normalized autocorrelation decays obtained with our Alexa555-labeled ssDNA 5mer as a function of total surfactant concentration. These data were acquired by spiking diluted vesicle samples with the dye-labeled DNA. The overall autocorrelation decay time increases with the total surfactant concentration due to electrostatic adsorption of DNA to the more slowly diffusing vesicles. Equation 5.3 was used to fit the data in Figure 5.2. At each surfactant concentration, the fraction of adsorbed dye was determined and an adsorption isotherm was obtained. In Figure 5.3, the isotherm for the 5mer is compared with isotherms for a 40mer ssDNA molecule and the small dye molecule, carboxyfluorescein. The isotherms are plotted

against the concentration of excess CTA^+ ions ($[CTA^+]_{excess}$) which provides a good estimation of the initial concentration of available electrostatic adsorption sites; adsorption at the surfactant vesicle interface occurs when charged groups on the solute form ion pairs with the excess surfactant in the vesicle bilayer. The solid lines in Figure 5.3 are fits to equation 5.4 and were used to obtain adsorption binding constants for the three probe molecules and these are reported in Table 5.1.
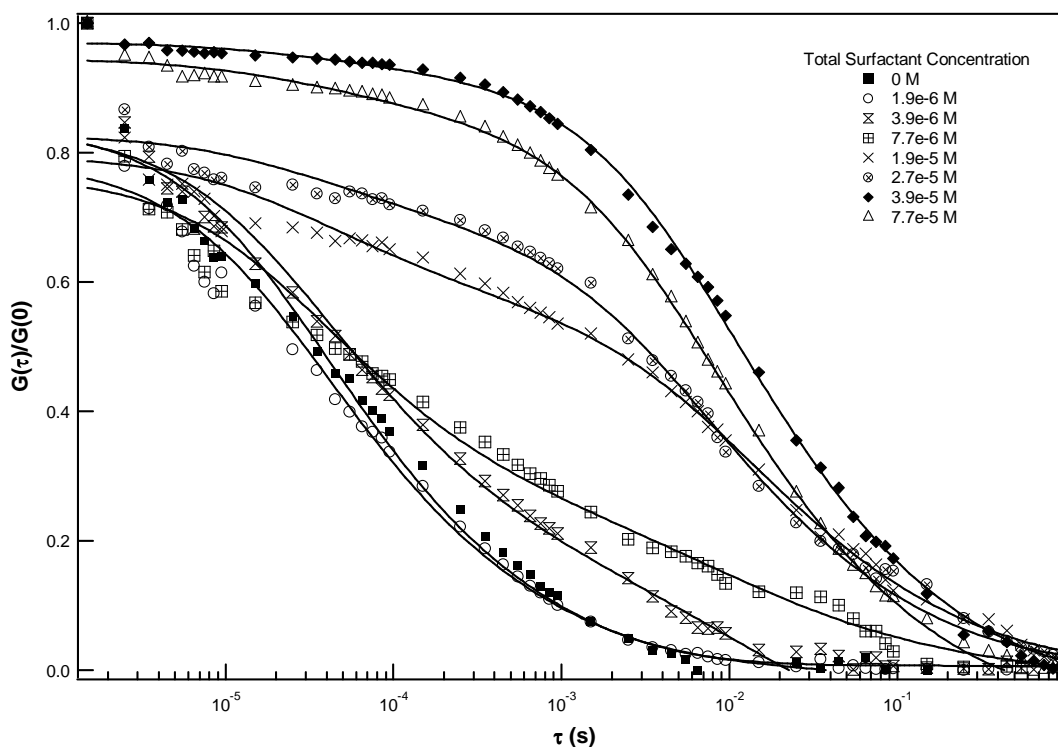
Figure 5.2 Normalized autocorrelation decays for 5mer ssDNA with varying surfactant concentrations
These autocorrelations are representative of data from one experiment.
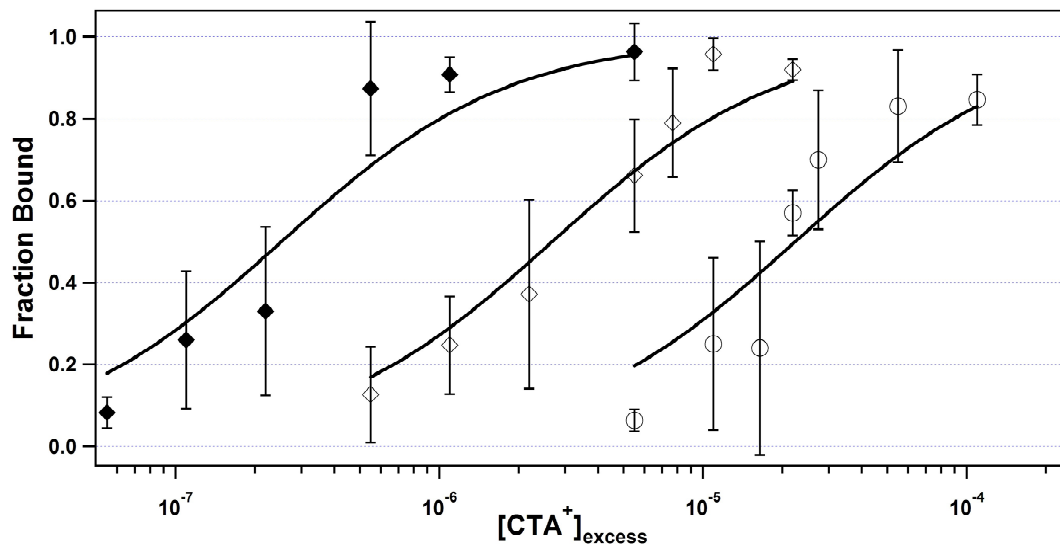
Figure 5.3 Adsorption isotherms for 40mer ssDNA, 5mer ssDNA, and CF
Adsorption isotherms obtained from fits of the autocorrelation decays. The 5mer ssDNA isotherm is in the center (open diamonds), the 40mer ssDNA isotherm is on the left (filled diamonds), and the CF isotherm is on the right (open circles). Error bars are one standard deviation around the mean value obtained for fraction bound at each surfactant concentration.

The binding constant and CTA^+ saturation concentration for the 5mer are an order of magnitude smaller than those of the ssDNA 40mer, reflecting a decrease in electrostatic binding due to the decreased number of charged groups on the 5mer. Likewise, the binding of the 5mer is an order of magnitude stronger than that of CF. CF and the 5mer are relatively similar in size, but have much different binding affinities due to the higher net charge of the 5mer. In addition to electrostatic interactions, hydrophobic and van der Waals interactions may contribute to the overall attraction. This is evidenced by variability in binding efficiencies of two molecules with the same net charge.[11] Hence, while electrostatic adsorption is the predominant driving force for molecular sequestration by catanionic vesicles, other forces and structural features come into play.

Sample	D (cm^{2}s^{-1})	K (M^{-1})
CF	1.5 x 10^{-6}	4.5 x 10^4
5mer	2.2 x 10^{-6}	3.7 x 10^5
40mer	7.5 x 10^{-7}	4.0 x 10^6

Table 5.1 Diffusion coefficients and binding constants for 5mer ssDNA, 40mer ssDNA, and CF
Diffusion coefficients for each probe molecule used in the study and binding constants for each probe
binding to CTAT-rich vesicles.

The two ssDNA samples provide an interesting comparison in which the predominant difference is the number of charges and size of the molecule. In addition to the increased number of charges, the 40mer is longer and can more easily span the distance between charge sites on the bilayer to facilitate multiple electrostatic interactions. For the surfactant composition used in these studies, CTAT is in 1.8-fold molar excess. Hence, if bilayer composition follows that of the bulk composition, the mole fraction of unpaired surfactant in the bilayer is $X_{CTA^+} = 0.44$. Walker and Zasadzinski previously reported the average head group areas in the CTA$^+$/DBS$^-$ bilayer to be 0.48 nm^2.[12] From these values one can estimate an average area per CTA$^+$ of 1.1 nm^2 and an average distance between CTA$^+$ sites of approximately 0.6 nm. The average distance between phosphates in ssDNA is approximately 6.3 Å,[13] so adjacent phosphates can span the same distance calculated between CTA$^+$ sites.

Figure 5.4 shows the binding isotherm for both DNA molecules plotted against the ratio of excess CTA$^+$ charge to total DNA charge, $R_{CTA}+$. The quantity $R_{CTA}+$ is calculated by

$$R_{CTA^+} = \frac{[CTA^+]-[DBS^-]}{[DNA]\times\{N_{nt}-1\}} \qquad (5.5)$$

where the quantities in square brackets denote molar concentrations and N_{nt} is the number of nucleotide bases, i.e. 5 or 40. There is a 100 fold difference in the saturation R_{CTA}^+ values for the two ssDNA samples. From Figure 5.4 it can be seen that binding saturation for the 40mer occurs at equimolar charge stoichiometry, i.e. when the total concentration of DNA phosphate charges and unpaired CTA^+ are equivalent. In contrast, saturation for the 5mer occurs when R_{CTA}^+ is >100, indicating that a much higher number of CTA^+ molecules is required to adsorb the smaller oligomer. This observation can be explained by considering the fact that the 40mer can span a much larger area on the bilayer interface and this facilitates more interactions between sparsely spaced CTA^+ ions. The 5mer can only interact with multiple CTA^+ that lie within a much smaller area of the vesicle bilayer.
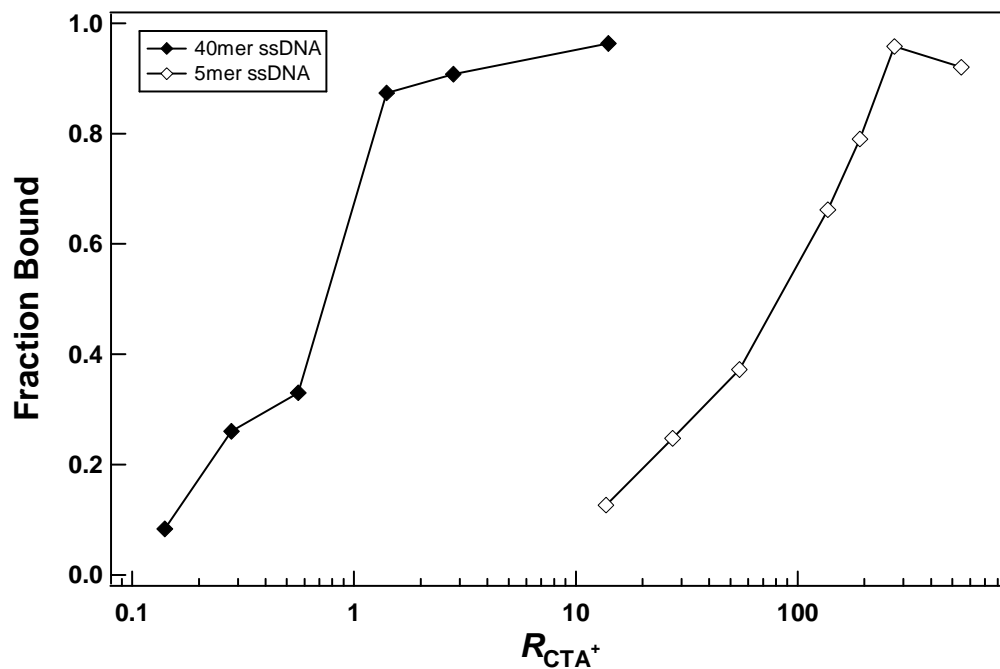
Figure 5.4 Adsorption isotherms of 5mer ssDNA and 40mer ssDNA
Adsorption isotherms are plotted against the ratio of excess CTA^+ charge to total DNA charge.

Since the length of the DNA strand is a factor in binding to catanionic surfactant vesicles, it was thought there could possibly be a difference between single stranded and double stranded DNA as well. Single stranded and double stranded DNA have different conformations in solution because double stranded DNA, if shorter than the persistence length (~150bp),[14,15] exists as a rigid rod while single stranded DNA in solution has flexibility in conformation. In order to compare single and double stranded DNA, a 40mer dsDNA was used to compare with the previous 40mer ssDNA data. The data appeared to have the same saturation point (not shown), and the resulting isotherm was nearly identical to the isotherm for 40mer ssDNA. The binding constant for 40mer dsDNA was 1.2×10^6 M^{-1}, compared to the value of 4.0×10^6 M^{-1} for 40mer ssDNA. Perhaps because the 40mer dsDNA exists in a rigid conformation, only one charged face of the DNA molecule could come in contact with the vesicle surface at a time. Therefore, the vesicle is binding to the same amount of charge as it does when the single stranded 40mer is bound, but the dsDNA experiences slightly lower binding affinity, most likely due to its diminished flexibility in comparison to ssDNA.

Because catanionic surfactant vesicles have potential as drug delivery and gene therapy agents, the interaction of dyes and DNA with vesicles was probed at physiological salt concentrations. The concentration of surfactant was maintained at the saturation point of the binding isotherm, the DNA or CF concentration was kept constant at 10nM, and the concentration of NaCl was varied. The results of the salt study with the 40mer and CF are shown in Figure 5.5, along with a salt study done for comparison purposes using SDBS-rich vesicles and rhodamine 6G (R6G). Both the

40mer and the CF "salted off" at an NaCl concentration of 0.1 M even though the 40mer has a larger negative charge and a larger binding constant. In contrast, binding of R6G to the SDBS-rich vesicles appears to be unaffected by increasing salt concentration, which brings into question the role of the counterion in the bilayer. In the SDBS-rich vesicles, the counterion in the majority is Na^+, so adding more sodium ions to these vesicles would not produce much of an affect on binding as sodium is already present in the Stern layer. In the CTAT-rich vesicles, the counterion in the majority is tosylate, an organic anion that can intercalate into the bilayer instead of just residing in the Stern layer. To test the role of the tosylate ion in cargo binding, CTAB-rich vesicles (cetyltrimethylammonium bromide) were substituted for CTAT-rich vesicles used in the binding study with the ssDNA 40mer (Fig. 5.5). The CTAB-rich vesicles gave the same result as the CTAT-rich vesicles: at normal saline levels, there was no 40mer ssDNA bound to the vesicles. Since the counterion does not appear to be a factor in cargo binding, it is possible that the "salting off" of the DNA is due to the loss of the entropic driving force for DNA binding.

In work by M.T. Record et al. on the binding of DNA to several types of ligands such as magnesium ions, polymers of the amino acid lysine, and the RNase enzyme, the driving force for the DNA binding process was determined to be the release of counterions bound to the DNA.[16] In addition, in studies of the nonspecific binding of the LacI protein from *E. coli* to DNA, it was determined that the binding could be modeled in the same manner.[17] The release of monovalent counterions from the DNA increased entropy, making it thermodynamically favorable for binding to occur. The observed binding was also found to be sensitive to the salt concentration

in solution. It was initially discovered by Latt and Sober that increasing the sodium ion concentration decreased the binding constant for DNA binding,[18] and was later corroborated by Record et al. in their DNA binding experiments.[16,17] This result mirrors what is seen in our experiments wherein the 5mer and 40mer appear to be "salted off" the surfactant vesicles. The electrostatic binding of the 5mer and 40mer must be driven by the release of counterions from the DNA and possibly the vesicles, and that process becomes less favorable as the NaCl concentration is increased, reducing the binding constant and producing the observed results that the DNA is no longer bound to vesicles at higher NaCl concentrations.
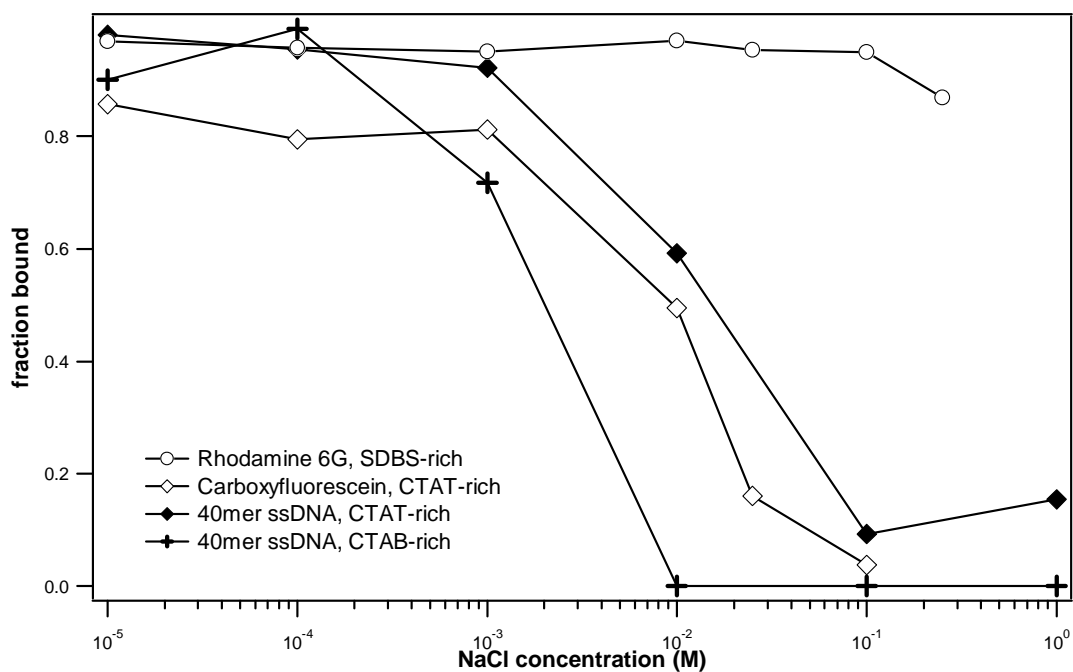
Figure 5.5 Salt study comparison
Salt studies for 40mer ssDNA with CTAT-rich vesicles and CTAB-rich vesicles, CF with CTAT-rich vesicles, and R6G with SDBS-rich vesicles.

5.5   *Conclusions*

In the binding isotherm study, it was determined that the length of a DNA molecule does affect binding affinity, while the difference between single stranded DNA and double stranded DNA in solution seems to have a much smaller effect on binding. This could change if the double stranded DNA becomes longer than the persistence length, as the DNA conformation will no longer be a rigid rod. With the results of these first experiments under physiological conditions, it appears as though CTAT-rich catanionic surfactant vesicles may not be able to retain their cargo molecules. More extensive studies will have to be done, especially in physiological buffered systems, as all these studies were performed in water purified by a Millipore system, which has a pH lower than 7. Other positively charged surfactants could be tested as well to determine if a different type of cation would produce stronger binding that would not be affected by an increased salt concentration.

References

1. Morgan, M. A.; Okamoto, K.; Kahn, J. D.; English, D. S., Single-molecule spectroscopic determination of lac repressor-DNA loop conformation. *Biophys. J.* **2005,** 89, (4), 2588-2596.

2. Pons, T.; Medintz, I. L.; Wang, X.; English, D. S.; Mattoussi, H., Solution-phase single quantum dot fluorescence resonance energy transfer. *J. Am. Chem. Soc.* **2006,** 128, (47), 15324-15331.

3. Elson, E. L.; Magde, D., Fluorescence correlation spectroscopy 1. Conceptual basis and theory. *Biopolymers* **1974,** 13, (1), 1-27.

4. Thompson, N. L., In *Topics in fluorescence spectroscopy*, Lakowicz, J. R., Ed. Plenum Press: New York, 1991; pp 337-378.

5. Moghimi, S. M.; Hunter, A. C.; Murray, J. C., Nanomedicine: Current status and future prospects. *FASEB J.* **2005,** 19, (3), 311-330.

6. Kaler, E. W.; Herrington, K. L.; Murthy, A. K.; Zasadzinski, J. A. N., Phase-behavior and structures of mixtures of anionic and cationic surfactants. *J. Phys. Chem.* **1992,** 96, (16), 6698-6707.

7. Kaler, E. W.; Murthy, A. K.; Rodriguez, B. E.; Zasadzinski, J. A. N., Spontaneous vesicle formation in aqueous mixtures of single-tailed surfactants. *Science* **1989,** 245, (4924), 1371-1374.

8. Safran, S. A.; Pincus, P.; Andelman, D., Theory of spontaneous vesicle formation in surfactant mixtures. *Science* **1990,** 248, (4953), 354-356.

9. Danoff, E. J.; Wang, X.; Tung, S. H.; Sinkov, N. A.; Kemme, A. M.; Raghavan, S. R.; English, D. S., Surfactant vesicles for high-efficiency

capture and separation of charged organic solutes. *Langmuir* **2007,** 23, (17), 8965-8971.

10. Wang, X.; Danoff, E. J.; Sinkov, N. A.; Lee, J.-H.; Raghavan, S. R.; English, D. S., Highly efficient capture and long-term encapsulation of dye by catanionic surfactant vesicles. *Langmuir* **2006,** 22, (15), 6461-6464.

11. Lioi, S. B.; Wang, X.; Islam, M. R.; English, D. S., Catanionic surfactant vesicles for electrostatic molecular sequestration and separation. *Phys. Chem. Chem. Phys.* **2009,** 11, 9315 - 9325.

12. Walker, S. A.; Zasadzinski, J. A., Electrostatic control of spontaneous vesicle aggregation. *Langmuir* **1997,** 13, (19), 5076-5081.

13. Murphy, M. C.; Rasnik, I.; Cheng, W.; Lohman, T. M.; Ha, T. J., Probing single-stranded DNA conformational flexibility using fluorescence spectroscopy. *Biophys. J.* **2004,** 86, (4), 2530-2537.

14. Borochov, N.; Eisenberg, H.; Kam, Z., Dependence of DNA conformation on the concentration of salt. *Biopolymers* **1981,** 20, (1), 231-235.

15. Godfrey, J. E.; Eisenberg, H., Flexibility of low-molecular weight double-stranded DNA as a function of length 2. Light-scattering measurements and estimation of persistence lengths from light-scattering, sedimentation and viscosity. *Biophys. Chem.* **1976,** 5, (3), 301-318.

16. Record, M. T.; Lohman, T. M.; Dehaseth, P., Ion effects on ligand-nucleic acid interactions. *J. Mol. Biol.* **1976,** 107, (2), 145-158.

17.   Dehaseth, P. L.; Lohman, T. M.; Record, M. T., Nonspecific interaction of lac

        repressor with DNA: An association reaction driven by counterion release.

        Biochemistry **1977,** 16, (22), 4783-4790.

18.   Latt, S. A.; Sober, H. A., Protein-nucleic acid interactions 2. Oligopeptide-

        polyribonucleotide binding studies. *Biochemistry* **1967,** 6, (10), 3293-3306.

Chapter 6:   Cell Viability Studies

6.1   Introduction

Surfactant vesicles have been proposed for use as drug delivery, gene therapy, and transfection agents. If CTAT/SDBS vesicles are to be used for this application, cell viability studies must be done to ensure that the surfactant vesicles will not harm cells. Previous toxicity studies showed that catanionic surfactant vesicles made from sodium dodecylsulfate (SDS) and hexadecyltrimethylammonium bromide (HTMAB) were indeed toxic to murine macrophage-like RAW cells.[1] To test the viability of cells exposed to CTAT/SDBS vesicles, two preparations of vesicles, SDBS micelles, and glucose modified surfactant vesicles[2,3] were tested on rat marrow stromal cells (MSC) and bovine chondrocyte cells.

6.2   Materials and Methods

6.2.1 Materials

The surfactants CTAT and SDBS were ordered from Aldrich Chemicals and were kept in a desiccator to prevent water absorption. Glucose modified surfactant *n*-dodecyl-β-d-glucopyranoside was purchased from Sigma. Rat marrow stromal cells and bovine chondrocyte cells were harvested in the laboratory of Dr. John Fisher of the University of Maryland. The Live/Dead Assay kit was purchased from Molecular Probes.

6.2.2 Vesicle Preparation

Vesicle samples were prepared at a total surfactant concentration of 1% by weight. Plain vesicle preparations used here were 7:3 and 3:7 CTAT:SDBS by weight. For the 7:3 CTAT:SDBS vesicles, 0.07 g CTAT and 0.03 g SDBS were weighed out and Millipore water was added to bring the total mass to 10 g. For the 3:7 CTAB:SDBS vesicles, 0.03 g CTAT and 0.07 g SDBS were weighed out and Millipore water was added to bring the total mass to 10 g. Glucose modified vesicles were made using two different mole fractions of glucose modified surfactant, and the amounts of CTAT and SDBS were adjusted so that the ratio of CTAT:SDBS was 3:7 and the total surfactant concentration was 1% by weight. SDBS micelles were made by weighing out 0.07 g of SDBS and adding 9.9 g of Millipore purified water so that the concentration of SDBS was the same as in the 7:3 SDBS:CTAT preparation. Vesicle and micelle solutions were stirred for several days to ensure surfactants had dissolved and equilibrium had been reached.

6.2.3 Cell Viability Determination

The two cell types (bovine chondrocyte cells and rat marrow stromal cells) used were incubated on a 96-well plate using DMEM (Dulbecco's Modified Eagle Medium) plus 10% FBS (Fetal Bovine Serum). Before incubating the vesicles with the cells, the vesicles were filtered through a 0.22 µm syringe filter and then diluted using the DMEM plus 10% FBS. The initial vesicle concentration as prepared was 1% w/w, and dilutions for incubating with the cells were made with this initial preparation and diluted using DMEM and 10% FBS. The dilutions for the vesicles were a series of 10-fold dilutions, so that the final concentrations for vesicles with the

cells were 0.1%, 0.01%, 0.001%, 0.0001%, 0.00001%, and 0.000001% w/w. The vesicles were incubated for 24 hours with the cells, and then the Live/Dead Assay (Invitrogen) was performed according to instructions that come with the kit. The Live/Dead Assay contains two dyes: calcein AM and ethidium homodimer, and the fluorescence of each molecule was used to determine the percentage of cells alive and the percentage of cells dead. Two reference samples were used to compare with the cells exposed to vesicles: living cells that only react with calcein AM to produce green fluorescence, and dead cells that only react with ethidium homodimer-1 to produce red fluorescence. After incubating the dyes for 30-45 minutes in all sample wells used on the 96 well plate, the fluorescence was read using a plate reader, and calculations were performed to determine the percentage of cells alive in each sample. The following equation was used to calculate the percentage of live cells

$$\% \text{ Alive} = \frac{F_{\text{sample}} - F_{\text{bckgd}}}{F_{\text{ref}} - F_{\text{bckgd}}} \tag{6.1}$$

The fluorescence was measured at 530 nm for each sample (F_{sample}), and the background fluorescence was subtracted (F_{bckgd}), which was then divided by the fluorescence of the live cell reference sample (F_{ref}) minus the background fluorescence (F_{bckgd}). The background fluorescence was obtained from the fluorescence at 530 nm for the dead cell reference sample, and the reference cell fluorescence was obtained from the fluorescence at 530 nm for the live cell reference sample. It is possible for the percentage of living cells to exceed 100% if the fluorescence of the sample was larger than the reference sample's fluorescence. The fluorescence for three individual samples of cells exposed to each surfactant

concentration was recorded, and the resulting percentages of living cells were averaged and error bars of one standard deviation around the average were calculated.

6.3   *Results and Discussion*

At surfactant concentrations of 0.001 mg/mL and below, cell viability is unaffected by SDBS-rich (V⁻) and CTAT-rich (V⁺) surfactant vesicles.   This concentration corresponds to a total surfactant concentration of 2.4 µM for CTAT-rich vesicles and 2.7 µM for SDBS-rich vesicles. From the fluorescence correlation spectroscopy (FCS) experiments shown in chapter 4, it has been shown that vesicles still exist at concentrations just below 2 µM. Because of this, we can be certain that vesicles are present at this concentration and the fact that cell viability is unaffected is encouraging. For some of the experiments, cell viability remains high at even higher concentrations of surfactant, indicating that it could be possible to utilize vesicles as drug delivery and transfection agents and not harm the cells.

There is, however, a difference in how the CTAT-rich vesicles and SDBS-rich vesicles affect the two different cell types tested, as seen in Figure 6.1. In both cell types, the CTAT-rich vesicles seem to affect cell viability more than the SDBS-rich vesicles do, but this result is more dramatic in the chondrocyte cells.   The chondrocytes are still viable at a total surfactant concentration of 27 µM for the SDBS-rich vesicles, while a total surfactant concentration of 24 µM for the CTAT-rich vesicles had no viable cells remaining. The viability of the marrow stromal cells is very similar for both the CTAT-rich and the SDBS-rich vesicles, and is only slightly less when exposed to the CTAT-rich vesicles. The cell viability could be

lower for CTAT-rich vesicles because the cells have an overall negative charge. The CTAT-rich vesicles have an overall positive charge, and would be more attracted to the cell surface than the negatively charged SDBS-rich vesicles. Because of this attractive force, the CTAT-rich vesicles may come into contact with cells more often and hence affect the viability more.
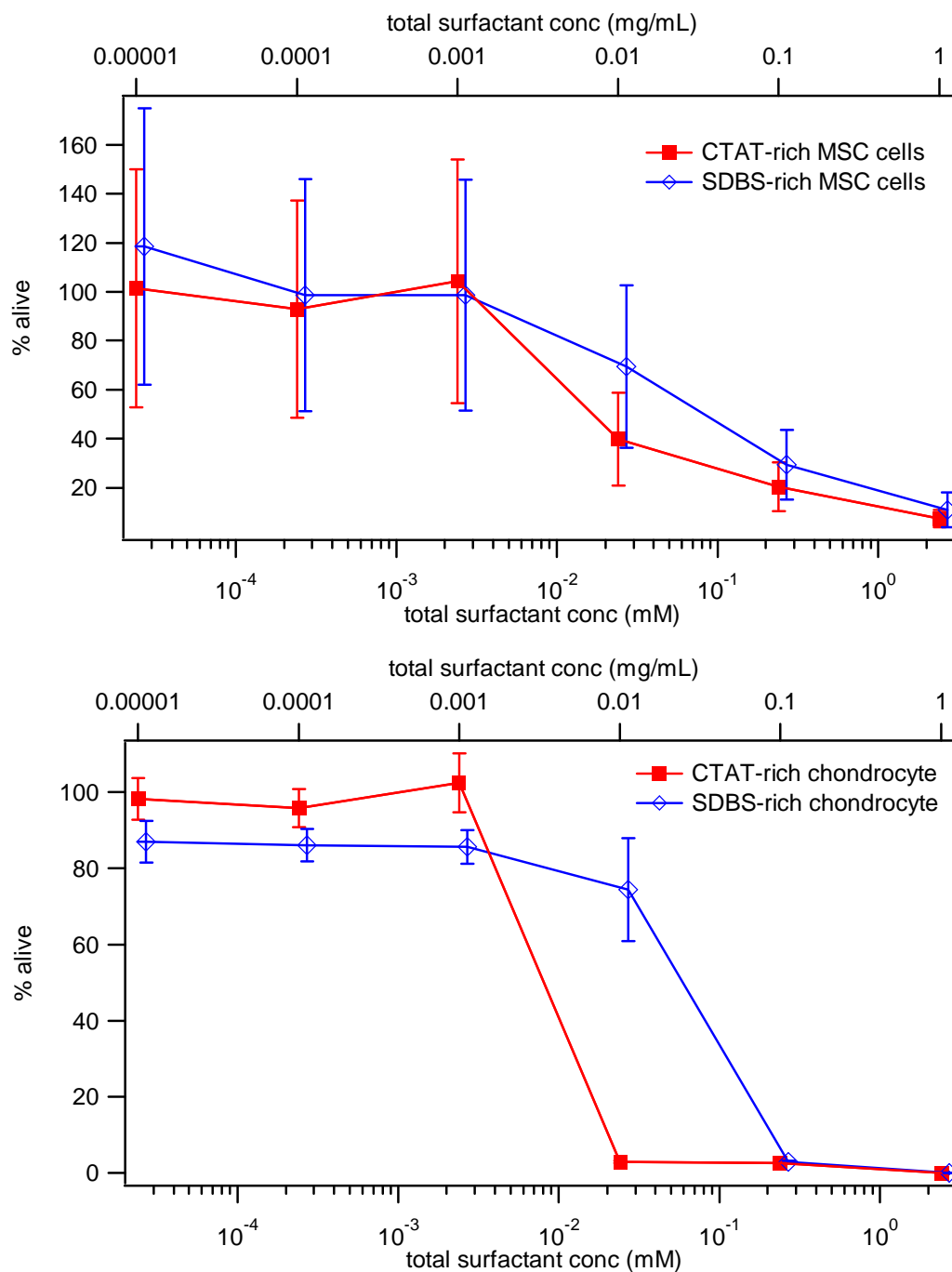
Figure 6.1 Cell viability with CTAT-rich vesicles and SDBS-rich vesicles
Cell viability of marrow stromal cells (top) and chondrocyte cells (bottom) when exposed to SDBS-rich vesicles and CTAT-rich vesicles.

Pure SDBS micelles were incubated with both cell types in order to test the affect of having positively charged surfactant present in the SDBS-rich vesicles. For both cell types, the SDBS-rich vesicles affected the cell viability more than the SDBS micelles. The cells were found to be basically immune to the SDBS micelles except at the very highest concentration of 2 mM (Fig. 6.2), where most likely any surfactant at that concentration would cause cell death. Even though the SDBS-rich vesicles have an overall negative charge, the positively charged CTAT surfactant present in those vesicles still appears to have an effect on cell viability.
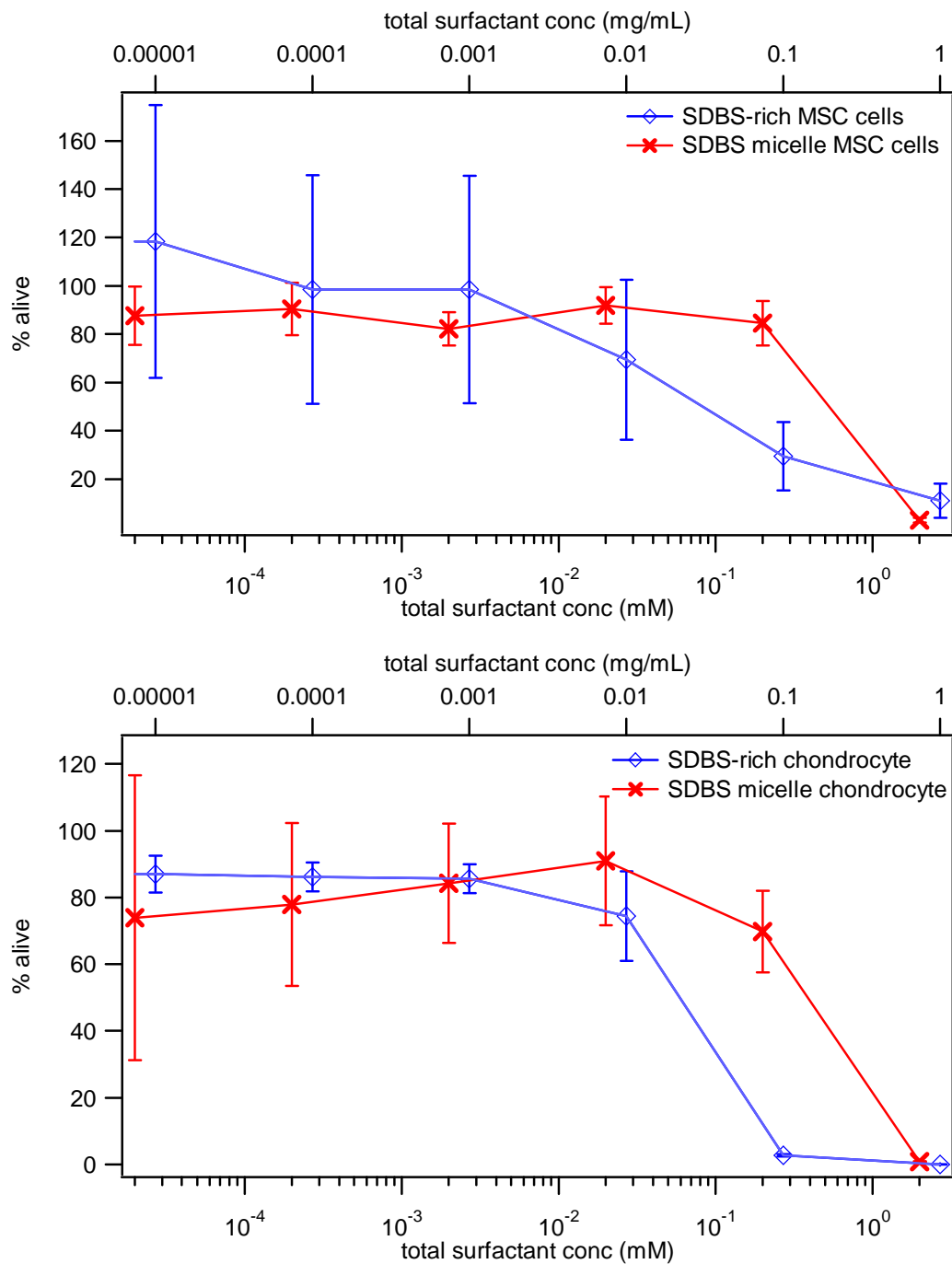
Figure 6.2 Cell viability with SDBS-rich vesicles and SDBS micelles
Cell viability of marrow stromal cells (top) and chondrocyte cells (bottom) when exposed to SDBS-rich vesicles and SDBS micelles.

Finally, SDBS-rich surfactant vesicles with glucose modified surfactants present at different mole fractions were tested and compared to the SDBS-rich vesicle results (Fig. 6.3). The cell viability for marrow stromal cells seemed to be affected more than the viability for chondrocyte cells. Even at very low concentrations of 0.2 mf glucose modified surfactant vesicles, the marrow stromal cell viability was at about 60%, but the chondrocyte cells exposed to very low concentrations of 0.2 mf glucose vesicles had a cell viability of higher than 80%. For the marrow stromal cells, the 0.01 mf glucose vesicles had cell viabilities around 80% at the lowest concentrations of surfactant tested, which was about the same for the chondrocyte cells. The cell viability for marrow stromal cells was different for each mole fraction of glucose modified surfactant vesicles compared to the pure SDBS-rich vesicles, while there was less of a difference in cell viability when chondrocyte cells were exposed to the pure SDBS-rich vesicles and SDBS-rich vesicles with glucose monomers. The 0.01 mf glucose vesicles had very little effect on the chondrocytes when compared to the plain SDBS-rich vesicles, while the 0.2 mf glucose vesicles had a visible difference when compared to the plain SDBS-rich vesicles. Both types of glucose vesicles have fewer surface charges than the pure SDBS-rich vesicles, so even with fewer charges interacting with the cells, the cell viability decreased. This could possibly indicate that the cells have glucose receptors, which would increase the likelihood of a vesicle interacting with a cell, thus decreasing cell viability when the cell is exposed to surfactant.

Figure 6.3 Cell viability with SDBS-rich vesicles and glucose modified SDBS-rich vesicles
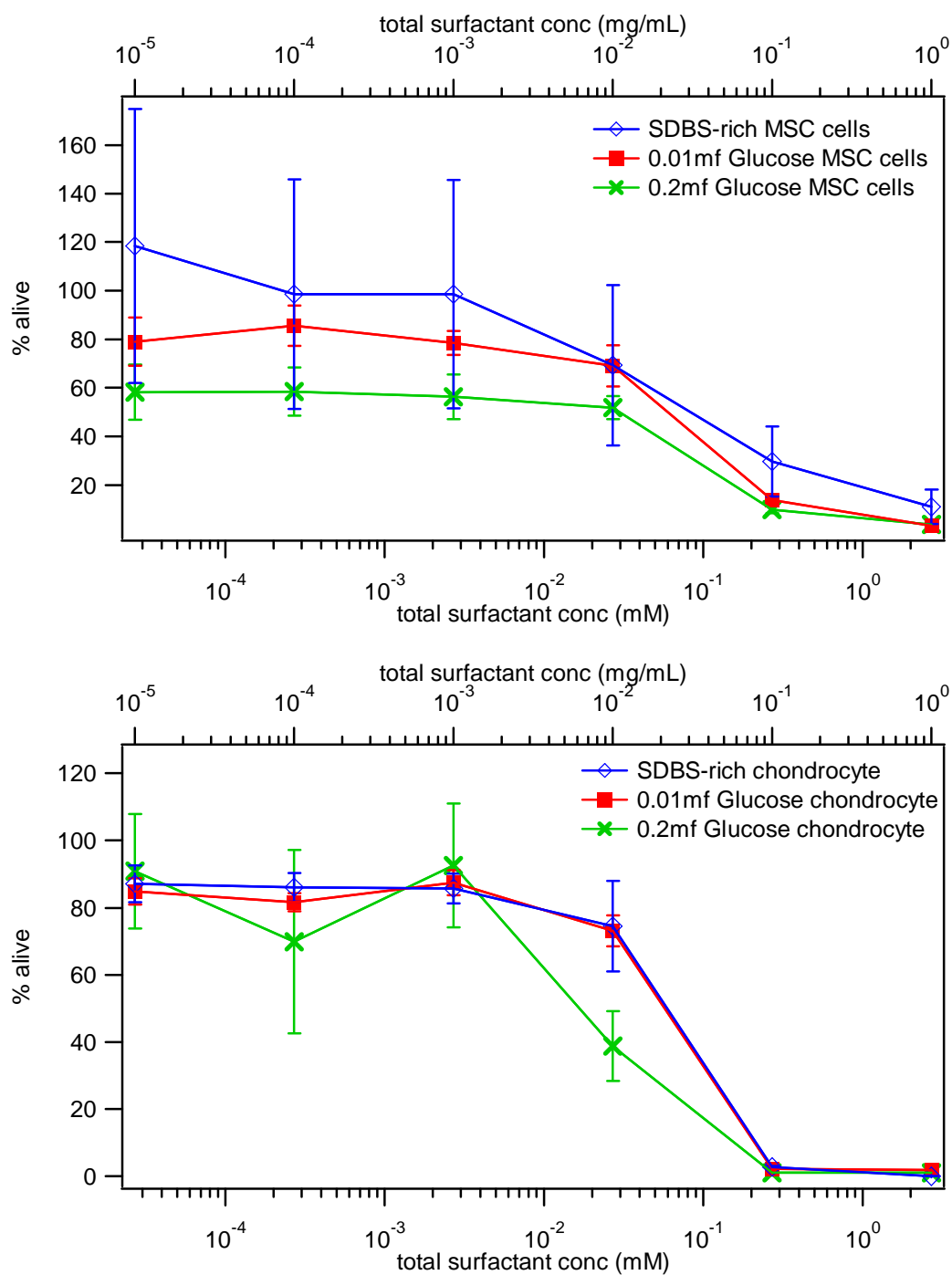Cell viability of marrow stromal cells (top) and chondrocyte cells (bottom) when exposed to SDBS-rich vesicles, SDBS-rich vesicles with 0.01mf glucose monomer, and SDBS-rich vesicles with 0.2mf glucose monomer.

6.4　*Conclusions*

Catanionic surfactant vesicles made from CTAT and SDBS could be used in application with live cells at low surfactant concentration because cell viability is high. However, because of results shown in chapter 5, the effects of normal saline would have to be overcome in order for the cargo molecule to remain on the exterior of CTAT-rich vesicles. If the cargo molecule is added to the surfactant solution before vesicles are formed, some of the cargo molecules would be encapsulated in the interior. Because these vesicles are more stable than traditional lipid vesicles, this preparation may still be a better alternative than lipid vesicle formulations. SDBS-rich vesicles maintain their cargo molecules in normal saline, but most likely would not fuse with cell membranes, as they both have the same overall charge and would repel each other. Modifications to surfactants such as adding glucose seem to have more of a negative effect on cell viability, suggesting that the cells might have glucose receptors in the outer leaflet of the bilayer. This result is promising in that vesicles could be targeted to certain cell types if the correct surfactant modification is made.

References

1. Kuo, J. H. S.; Jan, M. S.; Chang, C. H.; Chiu, H. W.; Li, C. T., Cytotoxicity characterization of catanionic vesicles in raw 264.7 murine macrophage-like cells. *Colloids and Surfaces B-Biointerfaces* **2005,** 41, (2-3), 189-196.

2. Park, J.; Rader, L. H.; Thomas, G. B.; Danoff, E. J.; English, D. S.; DeShong, P., Carbohydrate-functionalized catanionic surfactant vesicles: Preparation and lectin binding studies. *Soft Matter* **2008,** 4, 1916-1921.

3. Thomas, G. B.; Rader, L. H.; Park, J.; Abezgauz, L.; Danino, D.; DeShong, P.; English, D. S., Carbohydrate modified catanionic vesicles: Probing multivalent binding at the bilayer interface. *J. Am. Chem. Soc.* **2009,** 131, (15), 5471-5477.

Chapter 7:   Conclusions

Initial results of 40mer ssDNA binding to the exterior of CTAT-rich vesicles showed that the DNA binds much more strongly than small molecule organic dyes. A quantitative measure of DNA binding to catanionic surfactant vesicles had not previously been done, and in addition, none of the previous studies in the literature of DNA binding to surfactant vesicles used FCS. FCS has been shown to be a very sensitive technique for these studies, as a small 40mer ssDNA molecule can be differentiated from a small organic molecule fluorescent dye. It has also been shown that DNA may stabilize vesicle formation, as DNA bound to vesicles is seen at concentrations near the cac for CTAT/SDBS mixtures.

The strength of the interaction between DNA and surfactant vesicles is dependent upon the length of the DNA, but does not depend as strongly on whether the DNA is double stranded or single stranded. A small 5mer ssDNA bound less tightly than the 40mer ssDNA but more tightly than small molecule organic dyes. This indicates that the DNA can interact with more than one CTA^+ headgroup on the surface of the vesicle, and because the 40mer ssDNA is longer, it can have more interactions and bind more tightly than the 5mer ssDNA. A comparison of 40mer ssDNA to 40mer dsDNA yielded nearly identical values for the binding constant, but binding for the 40mer dsDNA was slightly lower because of its rigidity.

Subsequent salt studies of DNA bound to CTAT-rich vesicles showed that at normal saline conditions, the DNA is no longer bound to the vesicles but is free in

solution. The binding of small organic dye molecules to CTAT-rich vesicles had previously been shown to be to a lesser degree than binding of small organic dye molecules to SDBS-rich vesicles. This indicates that the interaction between the CTA^+ and the cargo molecule may be weaker, and if another smaller anion is introduced, that it would replace the DNA on the vesicle and the DNA is "salted off."

CTAT-rich vesicles may not be the best option for DNA delivery to cells unless the DNA is trapped on the interior of the vesicle as well. If the DNA were inside the vesicle, the normal saline concentrations would not affect the DNA and it could still be delivered to cells. The cell viability studies indicate that there is a chance of using CTAT-rich vesicles if the surfactant concentration is sufficiently low. Cells remained viable at low concentrations of surfactant, so they could be used for more than just DNA delivery; they could be useful in drug delivery as well. In addition, if surfactants are modified, as the glucose surfactants were, certain cell types could be targeted so that delivery of cargo molecules to those cell types is possible.

More experimentation could be performed to determine if the CTAT binding to cargo molecules is indeed weaker than SDBS binding to cargo molecules. A different positively charged surfactant could be used to create positively charged vesicles with SDBS, and binding studies could be done on the same small organic molecule fluorescent dyes used in previous studies and the DNA molecules used in this current study. In addition, salt studies could be done to determine if the CTA^+ ion affects the binding under normal saline conditions. It is important to determine binding under normal saline conditions, but it is important to perform experiments with physiological buffer systems as well since cellular conditions are most often at

neutral pH. Catanionic surfactant vesicles could still be very useful in biotechnological applications, but more experimentation will have to be done to determine if they are useful under the correct conditions for the application.

Chapter 8: Bibliography

1. Tadros, T. F., *Surfactants*. Academic Press, Inc.: New York, 1984.

2. Kaler, E. W.; Murthy, A. K.; Rodriguez, B. E.; Zasadzinski, J. A. N., Spontaneous vesicle formation in aqueous mixtures of single-tailed surfactants. *Science* **1989,** 245, (4924), 1371-1374.

3. Holland, P. M., Modeling mixed surfactant systems: Basic introduction. In *Mixed surfactant systems*, Holland, P. M.; Rubingh, D. N., Eds. American Chemical Society: Washington, D.C., 1992; pp 31-44.

4. Holland, P. M.; Rubingh, D. N., Nonideal multicomponent mixed micelle model. *J. Phys. Chem.* **1983,** 87, (11), 1984-1990.

5. Israelachvilli, J. N.; Mitchell, D. J.; Ninham, B. W., Theory of self-assembly of hydrocarbon amphiphiles into micelles and bilayers. *J. Chem. Soc., Faraday Trans. 2* **1976,** 72, (9), 1525-1568.

6. Israelachvili, J. N.; Mitchell, D. J.; Ninham, B. W., Theory of self-assembly of lipid bilayers and vesicles. *Biochim. Biophys. Acta* **1977,** 470, (2), 185-201.

7. Pashley, R. M.; Karaman, M. E., *Applied colloid and surface chemistry*. John Wiley and Sons, Ltd.: New York, 2004.

8. Shikata, T.; Hirata, H.; Kotaka, T., Micelle formation of detergent molecules in aqueous-media - Viscoelastic properties of aqueous cetyltrimethylammonium bromide solutions. *Langmuir* **1987,** 3, (6), 1081-1086.

9.   Soltero, J. F. A.; Puig, J. E.; Manero, O., Rheology of the cetyltrimethylammonium tosilate-water system 2. Linear viscoelastic regime. *Langmuir* **1996,** 12, (11), 2654-2662.

10.   Chiruvolu, S.; Israelachvili, J. N.; Naranjo, E.; Xu, Z.; Zasadzinski, J. A.; Kaler, E. W.; Herrington, K. L., Measurement of forces between spontaneous vesicle-forming bilayers. *Langmuir* **1995,** 11, (11), 4256-4266.

11.   Safran, S. A.; Pincus, P.; Andelman, D., Theory of spontaneous vesicle formation in surfactant mixtures. *Science* **1990,** 248, (4953), 354-356.

12.   Bangham, A. D.; Horne, R. W., Negative staining of phospholipids and their structural modification by-surface active agents as observed in electron microscope. *J. Mol. Biol.* **1964,** 8, (5), 660-668.

13.   Bangham, A. D.; Standish, M. M.; Watkins, J. C., Diffusion of univalent ions across lamellae of swollen phospholipids. *J. Mol. Biol.* **1965,** 13, (1), 238-252.

14.   Papahadjopoulos, D., Phospholipid model membranes 3. Antagonistic effects of Ca^{2+} and local anesthetics on permeability of phosphatidylserine vesicles. *Biochim. Biophys. Acta* **1970,** 211, (3), 467-477.

15.   Hope, M. J.; Bally, M. B.; Webb, G.; Cullis, P. R., Production of large unilamellar vesicles by a rapid extrusion procedure - Characterization of size distribution, trapped volume and ability to maintain a membrane-potential. *Biochim. Biophys. Acta* **1985,** 812, (1), 55-65.

16.   Macdonald, R. C.; Macdonald, R. I.; Menco, B. P. M.; Takeshita, K.; Subbarao, N. K.; Hu, L. R., Small-volume extrusion apparatus for preparation

of large, unilamellar vesicles. *Biochim. Biophys. Acta* **1991,** 1061, (2), 297-303.

17. Poznansky, M. J.; Juliano, R. L., Biological approaches to the controlled delivery of drugs - A critical review. *Pharmacol. Rev.* **1984,** 36, (4), 277-336.

18. Danoff, E. J.; Wang, X.; Tung, S. H.; Sinkov, N. A.; Kemme, A. M.; Raghavan, S. R.; English, D. S., Surfactant vesicles for high-efficiency capture and separation of charged organic solutes. *Langmuir* **2007,** 23, (17), 8965-8971.

19. Wang, X.; Danoff, E. J.; Sinkov, N. A.; Lee, J.-H.; Raghavan, S. R.; English, D. S., Highly efficient capture and long-term encapsulation of dye by catanionic surfactant vesicles. *Langmuir* **2006,** 22, (15), 6461-6464.

20. Bramer, T.; Dew, N.; Edsman, K., Pharmaceutical applications for catanionic mixtures. *J. Pharm. Pharmacol.* **2007,** 59, (10), 1319-1334.

21. Caillet, C.; Hebrant, M.; Tondre, C., Sodium octyl sulfate/cetyltrimethylammonium bromide catanionic vesicles: Aggregate composition and probe encapsulation. *Langmuir* **2000,** 16, 9099-9102.

22. Kondo, Y.; Uchiyama, H.; Yoshino, N.; Nishiyama, K.; Abe, M., Spontaneous vesicle formation from aqueous-solutions of didodecyldimethylammonium bromide and sodium dodecyl-sulfate mixtures. *Langmuir* **1995,** 11, (7), 2380-2384.

23. Tondre, C.; Caillet, C., Properties of the amphiphilic films in mixed cationic/anionic vesicles: A comprehensive view from a literature analysis. *Adv. Colloid Interf. Sci.* **2001,** 93, 115-134.

24. Koehler, R. D.; Raghavan, S. R.; Kaler, E. W., Microstructure and dynamics of wormlike micellar solutions formed by mixing cationic and anionic surfactants. *J. Phys. Chem. B* **2000,** 104, (47), 11035-11044.

25. Kaler, E. W.; Herrington, K. L.; Murthy, A. K.; Zasadzinski, J. A. N., Phase-behavior and structures of mixtures of anionic and cationic surfactants. *J. Phys. Chem.* **1992,** 96, (16), 6698-6707.

26. Yaacob, II; Bose, A., An investigation of microstructures in cationic/anionic surfactant suspensions by cryogenic transmission electron microscopy. *J. Colloid Interf. Sci.* **1996,** 178, (2), 638-647.

27. Bhattacharya, S.; De, S. M.; Subramanian, M., Synthesis and vesicle formation from hybrid bolaphile/amphiphile ion-pairs. Evidence of membrane property modulation by molecular design. *J. Org. Chem.* **1998,** 63, (22), 7640-7651.

28. Fischer, A.; Hebrant, M.; Tondre, C., Glucose encapsulation in catanionic vesicles and kinetic study of the entrapment/release processes in the sodium dodecyl benzene sulfonate/cetyltrimethylammonium tosylate/water system. *J. Colloid Interf. Sci.* **2002,** 248, (1), 163-168.

29. Akao, T.; Fukumoto, A.; Ihara, H.; Ito, A., Conformational change in DNA induced by cationic bilayer membranes. *FEBS Lett.* **1996,** 391, (1-2), 215-218.

30. Kikuchi, I. S.; Carmona-Ribeiro, A. M., Interactions between DNA and synthetic cationic liposomes. *J. Phys. Chem. B* **2000,** 104, (13), 2829-2835.

31. Dias, R. S.; Lindman, B.; Miguel, M. G., Compaction and decompaction of DNA in the presence of catanionic amphiphile mixtures. *J. Phys. Chem. B* **2002,** 106, (48), 12608-12612.

32. Dias, R. S.; Pais, A.; Miguel, M. G.; Lindman, B., DNA and surfactants in bulk and at interfaces. *Colloids Surf., A* **2004,** 250, (1-3), 115-131.

33. Mel'nikov, S. M.; Dias, R.; Mel'nikova, Y. S.; Marques, E. F.; Miguel, M. G.; Lindman, B., DNA conformational dynamics in the presence of catanionic mixtures. *FEBS Lett.* **1999,** 453, (1,2), 113-118.

34. Rosa, M.; Miguel, M. D.; Lindman, B., DNA encapsulation by biocompatible catanionic vesicles. *J. Colloid Interf. Sci.* **2007,** 312, (1), 87-97.

35. Rosa, M.; Moran, M. D.; Miguel, M. D.; Lindman, B., The association of DNA and stable catanionic amino acid-based vesicles. *Colloids Surf., A* **2007,** 301, (1-3), 361-375.

36. Magde, D.; Webb, W. W.; Elson, E., Thermodynamic fluctuations in a reacting system - measurement by fluorescence correlation spectroscopy. *Phys. Rev. Lett.* **1972,** 29, (11), 705-708.

37. Magde, D.; Elson, E. L.; Webb, W. W., Fluorescence correlation spectroscopy 2. Experimental realization. *Biopolymers* **1974,** 13, (1), 29-61.

38. Elson, E. L.; Magde, D., Fluorescence correlation spectroscopy 1. Conceptual basis and theory. *Biopolymers* **1974,** 13, (1), 1-27.

39. Hess, S. T.; Huang, S. H.; Heikal, A. A.; Webb, W. W., Biological and chemical applications of fluorescence correlation spectroscopy: A review. *Biochemistry* **2002,** 41, (3), 697-705.

40. Berne, B. J.; Pecora, R., *Dynamic light scattering: With applications to chemistry, biology, and physics*. John Wiley & Sons, Inc.: New York, NY, 1976.

41. Aragon, S. R.; Pecora, R., Fluorescence correlation spectroscopy as a probe of molecular-dynamics. *J. Chem. Phys.* **1976,** 64, (4), 1791-1803.

42. Eigen, M.; Rigler, R., Sorting single molecules - Application to diagnostics and evolutionary biotechnology. *Proc. Natl. Acad. Sci. USA* **1994,** 91, (13), 5740-5747.

43. Koppel, D. E.; Axelrod, D.; Schlessinger, J.; Elson, E. L.; Webb, W. W., Dynamics of fluorescence marker concentration as a probe of mobility. *Biophys. J.* **1976,** 16, (11), 1315-1329.

44. Lioi, S. B. W., X.; Islam, M.R.; Danoff, E.J.; English, D.S., Catanionic surfactant vesicles for electrostatic molecular sequestration and encapsulation. *Phys. Chem. Chem. Phys.* **2009,** 11, 9315-9325.

45. Webb, W. W., Fluorescence correlation spectroscopy: Inception, biophysical experimentations, and prospectus. *Appl. Opt.* **2001,** 40, (24), 3969-3983.

46. Hess, S. T.; Heikal, A. A.; Webb, W. W., Fluorescence photoconversion kinetics in novel green fluorescent protein pH sensors (pHluorins). *J. Phys. Chem. B* **2004,** 108, (28), 10138-10148.

47. Lieto, A. M.; Cush, R. C.; Thompson, N. L., Ligand-receptor kinetics measured by total internal reflection with fluorescence correlation spectroscopy. *Biophys. J.* **2003,** 85, (5), 3294-3302.

48. Petrek, Z.; Schwille, P., Photobleaching in two-photon scanning fluorescence correlation spectroscopy. *Chemphyschem* **2008,** 9, (1), 147-158.

49. Gould, T. J.; Bewersdorf, J.; Hess, S. T., A quantitative comparison of the photophysical properties of selected quantum dots and organic fluorophores. *Z. Phys. Chem.* **2008,** 222, (5-6), 833-849.

50. Rochira, J. A.; Gudheti, M. V.; Gould, T. J.; Laughlin, R. R.; Nadeau, J. L.; Hess, S. T., Fluorescence intermittency limits brightness in CdSe/ZnS nanoparticles quantified by fluorescence correlation spectroscopy. *J. Phys. Chem. C* **2007,** 111, (4), 1695-1708.

51. Haupts, U.; Maiti, S.; Schwille, P.; Webb, W. W., Dynamics of fluorescence fluctuations in green fluorescent protein observed by fluorescence correlation spectroscopy. *Proc. Natl. Acad. Sci. USA* **1998,** 95, (23), 13573-13578.

52. Heikal, A. A.; Hess, S. T.; Webb, W. W., Multiphoton molecular spectroscopy and excited-state dynamics of enhanced green fluorescent protein (EGFP): Acid-base specificity. *Chem. Phys.* **2001,** 274, (1), 37-55.

53. Thompson, N. L.; Steele, B. L., Total internal reflection with fluorescence correlation spectroscopy. *Nat. Protoc.* **2007,** 2, (4), 878-890.

54. Allen, N. W.; Thompson, N. L., Ligand binding by estrogen receptor beta attached to nanospheres measured by fluorescence correlation spectroscopy. *Cytometry A* **2006,** 69A, (6), 524-532.

55. Larson, D. R.; Gosse, J. A.; Holowka, D. A.; Baird, B. A.; Webb, W. W., Temporally resolved interactions between antigen-stimulated IgE receptors and Lyn kinase on living cells. *J. Cell Biol.* **2005,** 171, (3), 527-536.

56.   Schwille, P.; Korlach, J.; Webb, W. W., Fluorescence correlation spectroscopy with single-molecule sensitivity on cell and model membranes. *Cytometry* **1999,** 36, (3), 176-182.

57.   Rusu, L.; Gambhir, A.; McLaughlin, S.; Radler, J., Fluorescence correlation spectroscopy studies of peptide and protein binding to phospholipid vesicles. *Biophys. J.* **2004,** 87, (2), 1044-1053.

58.   Horton, M. R.; Radler, J.; Gast, A. P., Phase behavior and the partitioning of caveolin-1 scaffolding domain peptides in model lipid bilayers. *J. Colloid Interf. Sci.* **2006,** 304, (1), 67-76.

59.   Eggeling, C.; Berger, S.; Brand, L.; Fries, J. R.; Schaffer, J.; Volkmer, A.; Seidel, C. A. M., Data registration and selective single-molecule analysis using multi-parameter fluorescence detection. *J. Biotechnol.* **2001,** 86, (3), 163-180.

60.   Wang, X. Study of electrostatic interaction between charged surfactant vesicles and ionic molecules by bulk and fluorescence correlation spectroscopy measurements. Ph.D. Dissertation, University of Maryland College Park, College Park, 2007.

61.   Morgan, M. A.; Okamoto, K.; Kahn, J. D.; English, D. S., Single-molecule spectroscopic determination of lac repressor-DNA loop conformation. *Biophys. J.* **2005,** 89, (4), 2588-2596.

62.   Pons, T.; Medintz, I. L.; Wang, X.; English, D. S.; Mattoussi, H., Solution-phase single quantum dot fluorescence resonance energy transfer. *J. Am. Chem. Soc.* **2006,** 128, (47), 15324-15331.

63.   Hess, S. T.; Webb, W. W., Focal volume optics and experimental artifacts in confocal fluorescence correlation spectroscopy. *Biophys. J.* **2002,** 83, (4), 2300-2317.

64.   Thompson, N. L., In *Topics in fluorescence spectroscopy*, Lakowicz, J. R., Ed. Plenum Press: New York, 1991; pp 337-378.

65.   Gregoriadis, G.; Florence, A. T., Liposomes in drug delivery - Clinical, diagnostic and ophthalmic potential. *Drugs* **1993,** 45, (1), 15-28.

66.   Moghimi, S. M.; Hunter, A. C.; Murray, J. C., Nanomedicine: Current status and future prospects. *FASEB J.* **2005,** 19, (3), 311-330.

67.   McKelvey, C. A.; Kaler, E. W.; Zasadzinski, J. A.; Coldren, B.; Jung, H. T., Templating hollow polymeric spheres from catanionic equilibrium vesicles: Synthesis and characterization. *Langmuir* **2000,** 16, (22), 8285-8290.

68.   Regev, O.; Marques, E. F.; Khan, A., Polymer-induced structural effects on catanionic vesicles: Formation of faceted vesicles, disks, and cross-links. *Langmuir* **1999,** 15, (2), 642-645.

69.   Walker, S. A.; Zasadzinski, J. A., Electrostatic control of spontaneous vesicle aggregation. *Langmuir* **1997,** 13, (19), 5076-5081.

70.   Lee, J. H.; Agarwal, V.; Bose, A.; Payne, G. F.; Raghavan, S. R., Transition from unilamellar to bilamellar vesicles induced by an amphiphilic biopolymer. *Phys. Rev. Lett.* **2006,** 96, (4).

71.   Kaler, E. W.; Herrington, K. L.; Miller, D. D.; Zasadzinski, J. A., Phase behavior of aqueous mixtures of anionic and cationic surfactants along a dilution path. In *Structure and dynamics of strongly interacting colloids and*

supramolecular aggregates in solution, Chen, S.-H.; Huang, J. S.; Tartaglia, P., Eds. Kluwer Academic Publishers: Dordrecht, 1992; Vol. 369. pp 571-577.

72.   Bonincontro, A.; Falivene, M.; La Mesa, C.; Risuleo, G.; Pena, M. R., Dynamics of DNA adsorption on and release from SDS-DDAB cat-anionic vesicles: A multitechnique study. *Langmuir* **2008,** 24, (5), 1973-1978.

73.   Bonincontro, A.; La Mesa, C.; Proietti, C.; Risuleo, G., A biophysical investigation on the binding and controlled DNA release in a cetyltrimethylammonium bromide-sodium octyl sulfate cat-anionic vesicle system. *Biomacromolecules* **2007,** 8, (6), 1824-1829.

74.   Dias, R. S.; Lindman, B.; Miguel, M. G., DNA interaction with catanionic vesicles. *J. Phys. Chem. B* **2002,** 106, (48), 12600-12607.

75.   Guo, X.; Li, H.; Zhang, F. M.; Zheng, S. Y.; Guo, R., Aggregation of single-chained cationic surfactant molecules into vesicles induced by oligonucleotide. *J. Colloid Interf. Sci.* **2008,** 324, (1-2), 185-191.

76.   Maeda, H.; Greish, K.; Fang, J., The EPR effect and polymeric drugs: A paradigm shift for cancer chemotherapy in the 21st century. In *Advances in polymer science*, Springer-Verlag Berlin: Berlin, 2006; Vol. 193, pp 103-121.

77.   Murphy, M. C.; Rasnik, I.; Cheng, W.; Lohman, T. M.; Ha, T. J., Probing single-stranded DNA conformational flexibility using fluorescence spectroscopy. *Biophys. J.* **2004,** 86, (4), 2530-2537.

78.   Borochov, N.; Eisenberg, H.; Kam, Z., Dependence of DNA conformation on the concentration of salt. *Biopolymers* **1981,** 20, (1), 231-235.

79.   Godfrey, J. E.; Eisenberg, H., Flexibility of low-molecular weight double-stranded DNA as a function of length 2. Light-scattering measurements and estimation of persistence lengths from light-scattering, sedimentation and viscosity. *Biophys. Chem.* **1976,** 5, (3), 301-318.

80.   Record, M. T.; Lohman, T. M.; Dehaseth, P., Ion effects on ligand-nucleic acid interactions. *J. Mol. Biol.* **1976,** 107, (2), 145-158.

81.   Dehaseth, P. L.; Lohman, T. M.; Record, M. T., Nonspecific interaction of lac repressor with DNA: An association reaction driven by counterion release. *Biochemistry* **1977,** 16, (22), 4783-4790.

82.   Latt, S. A.; Sober, H. A., Protein-nucleic acid interactions 2. Oligopeptide-polyribonucleotide binding studies. *Biochemistry* **1967,** 6, (10), 3293-3306.

83.   Kuo, J. H. S.; Jan, M. S.; Chang, C. H.; Chiu, H. W.; Li, C. T., Cytotoxicity characterization of catanionic vesicles in raw 264.7 murine macrophage-like cells. *Colloids Surf., B* **2005,** 41, (2-3), 189-196.

84.   Park, J.; Rader, L. H.; Thomas, G. B.; Danoff, E. J.; English, D. S.; DeShong, P., Carbohydrate-functionalized catanionic surfactant vesicles: Preparation and lectin binding studies. *Soft Matter* **2008,** 4, 1916-1921.

85.   Thomas, G. B.; Rader, L. H.; Park, J.; Abezgauz, L.; Danino, D.; DeShong, P.; English, D. S., Carbohydrate modified catanionic vesicles: Probing multivalent binding at the bilayer interface. *J. Am. Chem. Soc.* **2009,** 131, (15), 5471-5477.